Koninklijke Sterrenwacht van België
Observatoire royal de Belgique
Royal Observatory of Belgium

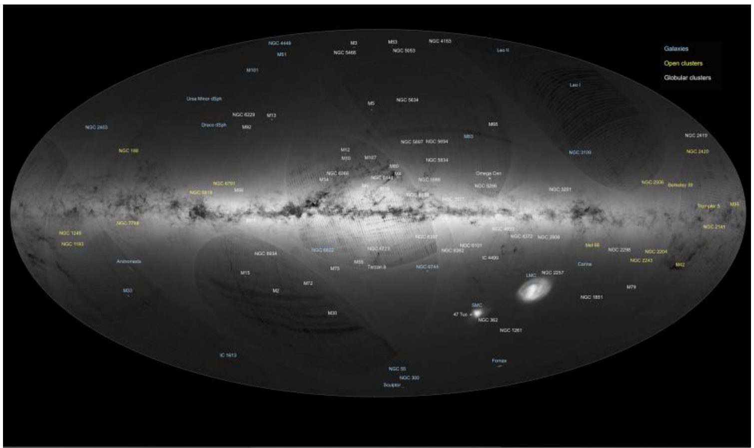

Jaarverslag 2017
Rapport Annuel 2017
Annual Report 2017

Cover illustration: ***Above: One billion star map of our galaxy created with the optical telescope of the satellite Gaia (Credit: ESA/Gaia/DPAC). Below: Three armillary spheres designed by Jérôme de Lalande in 1775. Left: the spherical sphere; in the centre: the geocentric model of our solar system (with the Earth in the centre); right: the heliocentric model of our solar system (with the Sun in the centre).***

De activiteiten beschreven in dit verslag werden ondersteund door
Les activités décrites dans ce rapport ont été soutenues par
The activities described in this report were supported by

De POD Wetenschapsbeleid
Le SPP Politique Scientifique
The Belgian Science Policy

De Nationale Loterij
La Loterie Nationale
The National Lottery

Het Europees Ruimtevaartagentschap
L'Agence Spatiale Européenne
The European Space Agency

De Europese Gemeenschap
La Communauté Européenne
The European Community

Het Fonds voor Wetenschappelijk Onderzoek – Vlaanderen

Le Fonds de la Recherche Scientifique

Table of contents

Preface

This report describes the highlights of scientific activities and public services at the Royal Observatory of Belgium in 2017.
A list of publications and the list of personnel are included at the end.
Due to lack of means and personnel the report is only in English.
If you need more or other information on the Royal Observatory of the Belgium and/or its activities please contact rob_info@oma.be *or visit our website* http://www.astro.oma.be.

Ronald Van der Linden
Director General

Reference Systems and Planetology

This Operational Directorate "Reference Systems and Planetology" contributes to the elaboration of reference systems and timescales, integrates Belgium in the international reference frames, and studies the interior, rotation, dynamics, and crustal deformation of the Earth and other terrestrial planets and moons of our solar system

The principal activities are grouped into two general themes:

1. *Space geodesy and timescales with GNSS (Global Navigation Satellite System), and*
2. *Rotation and interior structure of the Earth and other terrestrial planets and satellites.*

Global Navigation Satellite System (GNSS)

European Plate Observing System – EPOS

The ambition

Understanding how the Earth works as a system is critically important to modern society. Volcanic eruptions, earthquakes, floods, landslides, tsunamis, weather, and global climate change are all Earth phenomena affecting society.

How can we better understand these phenomena? How can we understand more about the chemical and physical processes responsible for these phenomena? How can we take measures to prevent the effect of these phenomena on the environment? Can we predict them?

Solid Earth science is the place where to find answers to these questions. Solid Earth science brings together many diverse disciplines such as geology, seismology, geodesy, volcanology, geomagnetism as well as chemistry and physics as they all apply to the workings of the Earth. The Royal Observatory of Belgium touches several of these disciplines, and corroborates that progress in solid Earth science relies on the integration of harmonized multidisciplinary, freely accessible, data and products which are – and here is the difficulty – originally generated by different communities with different data formats and processing procedures.

It is exactly the ambition of European Plate Observing System (EPOS) to offer a collaborative framework to provide, through a unique portal, open access to these multidisciplinary data as well as visualization and modelling tools.

The construction

Supported by the European Commission H2020 EPOS Implementation Phase Project, 47 partners, amongst which the Royal Observatory of Belgium, plus 6 associate partners from 25 countries from all over Europe and several international organizations (ORFEUS, EUREF, EMSC) are building up EPOS today. EPOS is expected to be operational from 2019 when it will become a European Research Infrastructure Consortium (ERIC) and thus a legal entity.

The Royal Observatory of Belgium participates more specifically to the GNSS Thematic Core Service that will provide access to GNSS data and their derived ground movements measured by thousands of GNSS stations all over Europe. We define and implement, together with European key players, the GNSS services that will run from 2019 on.

Link with EUREF

The involvement of the Royal Observatory of Belgium in EPOS is a natural follow up of our 20 years of commitment as Central Bureau of the EUREF Permanent GNSS Network (EPN). The EPN consists of 320 GNSS stations from 30+ European countries and provides access to the European Terrestrial Reference System 89 (ETRS89), which is the standard precise GNSS coordinate system throughout Europe. The Royal Observatory of Belgium acts as liaison between EPN station operators and analysis centers, maintains the network operation guidelines, provides the necessary station configuration metadata, and ensures the GNSS datasets meet the requirements of the analysis.

The Royal Observatory of Belgium ensures now the link between EUREF and EPOS. To support this, in 2017, we started the development of a new “Metadata Management and Dissemination System for Multiple GNSS Networks” (M3G, see Figure below). M3G will be used within both EUREF and EPOS. It will guarantee the consistency of the metadata available in both networks and facilitate the provision of EPN data to the EPOS Data Gateway (see Figure below). In 2017, M3G has already been successfully used in EPOS for demonstration purposes. In addition, we wrote dedicated operation guidelines for EPOS GNSS stations and maximized their harmonization with the existing EUREF standards.

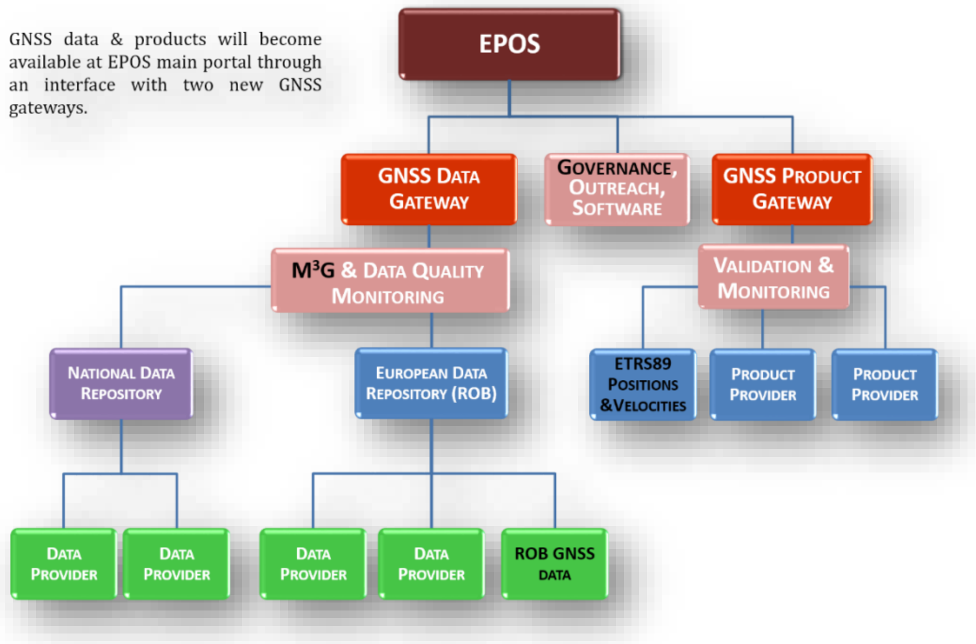

Schematic overview of the EPOS services that are designed by the GNSS Thematic Core Service. The activities indicated in black are the ones that the Royal Observatory of Belgium is already running in 2017. In 2018-2018, we will in addition 1) install the interface between our EPN GNSS data repository and EPOS, 2) set up GNSS data quality monitoring procedures similar to the procedures used today in the EPN

The success of EPOS depends for a large part on the amount of data and products that are made available by National Research Infrastructure (NRI, see Figure above) and international organizations, such as EUREF. The Royal Observatory of Belgium is an example of such an NRI and we will make our GNSS data available to EPOS and also act as the European data repository that makes available GNSS data from the EPN stations to EPOS. Today, the Royal Observatory of Belgium uses its extensive network of contacts to stimulate other National Research Infrastructures throughout Europe to contribute with their GNSS data to EPOS.

To maintain the ETRS89, EUREF computes multi-year coordinates/velocities of the EPN stations. They are regularly updated (each 15 weeks) and it is the core product of EUREF. Since the spring of 2017, The Royal Observatory of Belgium is responsible for computing this multi-year coordinates/velocities solution. Because the associated velocity field and position times series are valuable for geophysical research, ROB provides this solution also to the GNSS Product Gateway (see Figure above) of EPOS.

Time – Time Transfer

Precise timescale

On October 13th, 2017, we celebrated the 50th birthday of the atomic definition of the second as time unit. This means also that for 50 years, the Royal Observatory of Belgium is participating to the atomic realization of the time.

The official time in the world is the Universal Time Coordinated. It corresponds to a weighted average of atomic clocks distributed in about 60 time laboratories around the world, among which the Royal Observatory of Belgium. Being based on an ensemble of clocks, UTC is not available in real time and each time laboratory has to generate a physical realization of UTC to be disseminated to the users. The Royal Observatory of Belgium realization of UTC is named UTC(ORB), and is maintained through a Hydrogen Maser (a particular type of atomic clock) aligned on UTC with a dedicated algorithm. UTC(ORB) is then disseminated to the users via the Network Time Protocol.

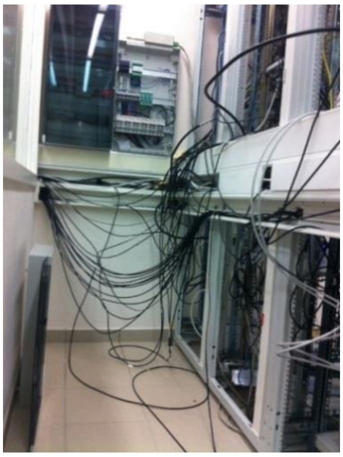

View of the ROB Time Laboratory in January 2017 (left) and December 2017 (right); a surge protection system was installed in 2017 through the metallic plate visible on the lower part of the wall in the picture on the right hand side

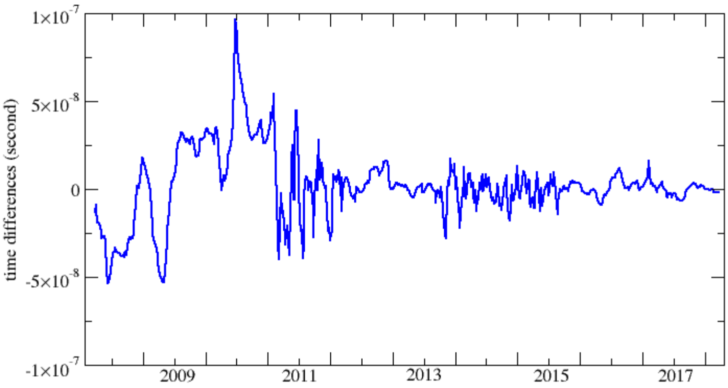

Difference between the realization UTC(ORB) and the true UTC during the last ten years

The quality of UTC(ORB) is continuously improving thanks to new calibration of the equipment, continuous upgrade of the time laboratory (see Figure above) and tight control procedures. During 2017, UTC(ORB) was realized with a very high quality, as not deviating from UTC by more than 7 nanosecond, as seen in the figure below which presents the difference UTC-UTC(ORB) over the last ten years. Thanks to this high quality, UTC(ORB) is also used since a few years by the European Agencies for the calibration and the monitoring of UTC disseminated by Galileo and EGNOS.

Earth Rotation, Geodesy and Geophysics of Terrestrial Planets

Investigation of the core of Mars from radio links between a Martian lander and the Earth

In 2020, ESA and the Russian space agency Roscosmos will launch the ExoMars 2020 mission. It consists of a rover with a lander platform that will land on Mars. Belgium contributes to one of the platform science instruments, a radio transponder with antennas called **LaRa** (Lander Radioscience). LaRa will receive radio signals of a fixed and very stable frequency in X-band from the Earth and send them back to Earth at a slightly different frequency without adding any instrumental phase (see figure below). On Earth, the Doppler shift on these signals will be measured by very large antennas in order to study the rotation of Mars. By characterizing its rotation variations, new information will be obtained about the core of Mars and about global changes in its atmosphere.

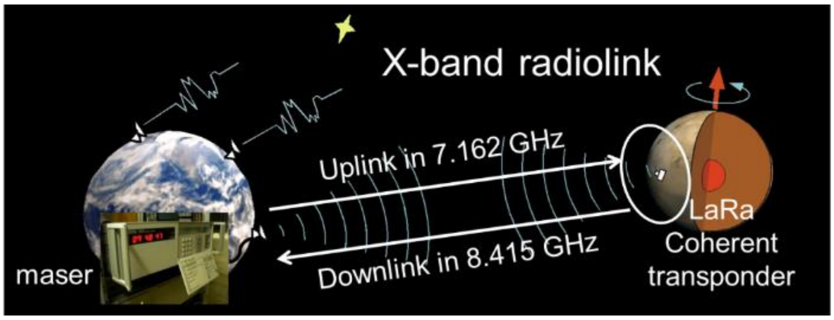

Principle of the LaRa experiment

The LaRa transponder is being designed and built by the Belgian company AntwerpSpace and the antennas by the Université catholique de Louvain (UCLouvain). The thermal and structural models (see figure below) as well as the interface simulator were delivered to the Russian partners in 2017. A ground station compatibility test has been performed at ESOC (European Space Operations Centre, in Darmstadt) imitating the Deep Space Network ground stations. The results shown that the performances of the transponder are even better than expected.

Structural model of LaRa

The Royal Observatory of Belgium also participates in the similar radio science experiment RISE (Rotation and Interior Structure Experiment) on the NASA mission InSight (launch on May 2018). Both experiments can observe Mars rotation changes through their effects on the position of a lander fixed on the surface of Mars. Different aspects of Mars rotation affect the position of a lander: nutations (periodic variations of Mars orientation in space), precession (long-term variation of Mars orientation in space), length-of-day (LOD) variations (changes in Mars rotation speed) and polar motion (variations of the rotation axis with respect to the pole). These motions have different signatures in the Doppler measurements between the Earth antennas and a Martian lander. In order to develop observation strategies that maximize the geophysical return, we studied the variations in the different Doppler signatures and the correlations between them as a function of time (see figure below).

Those Doppler signatures depend on the diurnal rotation of Mars, the lander position, the position of the Earth with respect to the equatorial plane of Mars and the considered variable (nutation, LOD or polar motion). As an example, the figure below shows that the nutation signature is proportional to the Earth declination. This information helps to identify the periods in which the nutation signature will be maximized or close to zero (see the gray boxes on the figure below), and to optimize the measurements for a maximal scientific return on the rotation and interior structure of Mars.

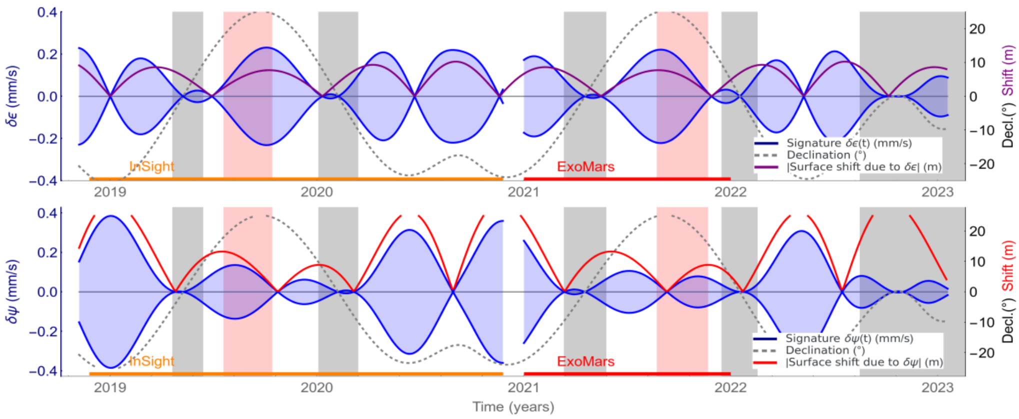

Signature of the nutations in longitude dy and in obliquity de in the Doppler observable as a function of time. The blue lines show the maximal and minimal nutation signatures each day. The grey boxes correspond to time intervals where the Earth declination is smaller than 10°, which means that the sensitivity to Mars spin axis motion in space is smaller. The pink boxes correspond to time intervals where the Sun-Earth-Probe (SEP) angle < 15°, which means that the data have a large noise due to the solar plasma

For an equatorial lander on Mars, the largest signatures in the Doppler observable are for the LOD variations, precession rate and nutation amplitudes. The polar motion and the nutation signatures related to the liquid core have a much smaller amplitude. For a lander closer to the pole, the polar motion signature is enhanced while the other signatures decrease. Since the Doppler observable is proportional to the time derivative of the distance between the emitter and the receiver and since the diurnal rotation is the largest frequency in this problem, all rotation signatures show variations at a Martian diurnal frequency (blue area in the figure above). The nutation signature varies at the sidereal diurnal frequency while the LOD signature oscillates at the solar diurnal frequency. This leads to a long-term shift between the two signatures, which can be used to de-correlate the rotation parameters. Another consequence is the increase of the LOD signature with increasing Earth elevation in the lander's sky, while the nutation signature is independent of the elevation.

We also studied the situation in which the Martian lander is tracked by an orbiting spacecraft. The lander-orbiter Doppler observable is more sensitive to the rotation parameters than the lander-Earth Doppler observable because of a shorter distance between the emitter and the receiver and because of the faster angular velocity of the orbiter. The advantages of this link are a larger signature by at least one order of magnitude for an orbiting spacecraft 500 km above the surface, more differences in geometry for the passes and another correlation pattern between the adjusted parameters.

Enceladus's non-uniform shell

The Saturn's moon Enceladus is the most geologically active icy satellite in the Solar System. Surprisingly, its activity is concentrated in the south pole where four long parallel cracks (`tiger stripes') emit jets of water vapour and icy particles (see figure below), as well as gigawatts of heat. These phenomena and the analysis of the plume composition point to the existence of a subsurface reservoir of liquid salt water. Tides due to orbital eccentricity were thought to be the culprit, but we still do not know why geysers only occur at the south pole, which mechanism controls their emission, and how a so small body can lose all that heat into space without freezing and thus ending tectonic activity.

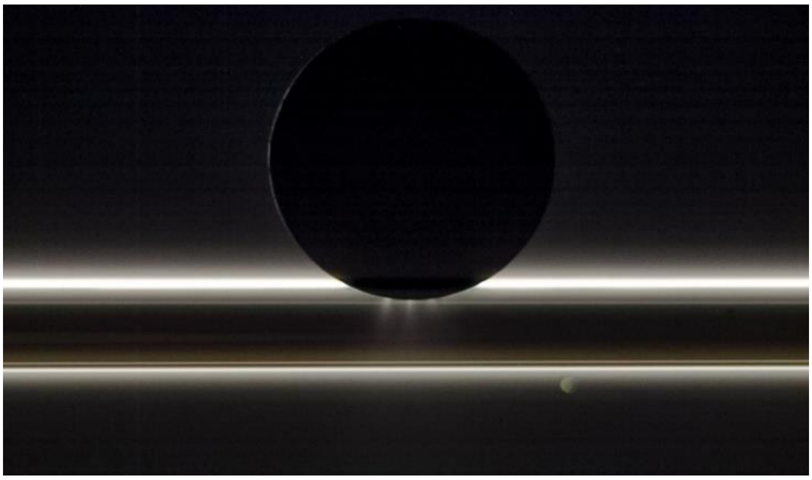

Saturn's moon Enceladus drifts before the rings and the tiny moon Pandora in this view captured by NASA's Cassini spacecraft on Nov. 1, 2009. The entire scene is backlit by the Sun, providing striking illumination for the icy particles that make up both the rings and the jets emanating from the south pole of Enceladus (PIA17144, NASA/JPL-Caltech/Space Science Institute)

Our knowledge of Enceladus interior has much evolved in the last three years. In particular, the detection of large libration – variations in the rotation rate – showed that the crust is uncoupled from the core by a global ocean and that it is much thinner than initially concluded from gravity data alone. In 2017, a team from the Royal Observatory made a new analysis of the libration and gravity data in order to obtain the most stringent constraints to date on the average thickness of the crust and its lateral thickness variations (see figure below). The average thickness of the crust is estimated to be 20 ± 1 km (locally 3 km at the south pole, 15 ± 2 km at the north pole), and the ocean depth 36 ± 2 km.

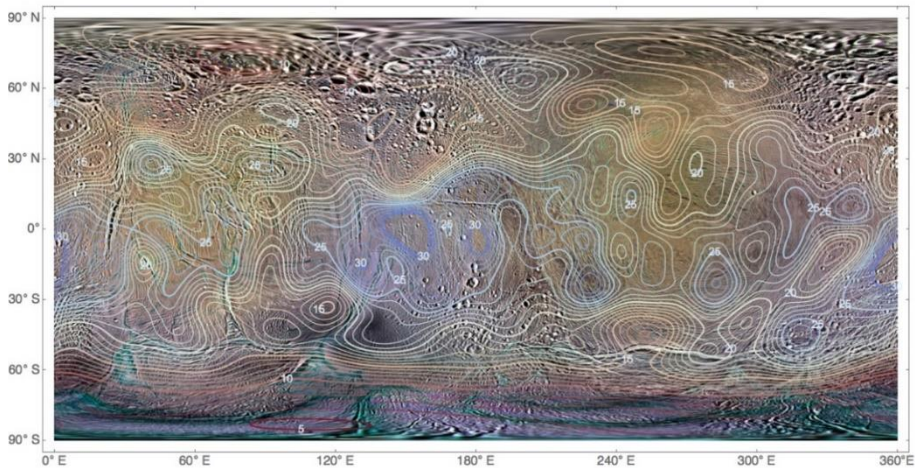

Thickness of Enceladus's crust (contours in km), superimposed on a global colour mosaic of the surface

Strong lateral variations of crustal thickness strongly affect the distribution of tidal stresses and must play a crucial role in the localization of geologic activity at the south pole of Enceladus. Predicting tidal deformations of a crust of non-uniform thickness has proven to be a challenge because methods previously developed for the Earth are not suited to icy moons with floating shells. We constructed a new theory to calculate tidal deformations of a non-uniform viscoelastic thin shell, allowing for large lateral variations of crustal thickness as well as large 3D variations of crustal rheology. The resulting tidal thin shell equations can be solved numerically much faster than 3D finite element methods. They also take into account effects that are often not included in finite element methods, such as self-gravity, density stratification below the shell, core viscoelasticity, and crustal compressibility.

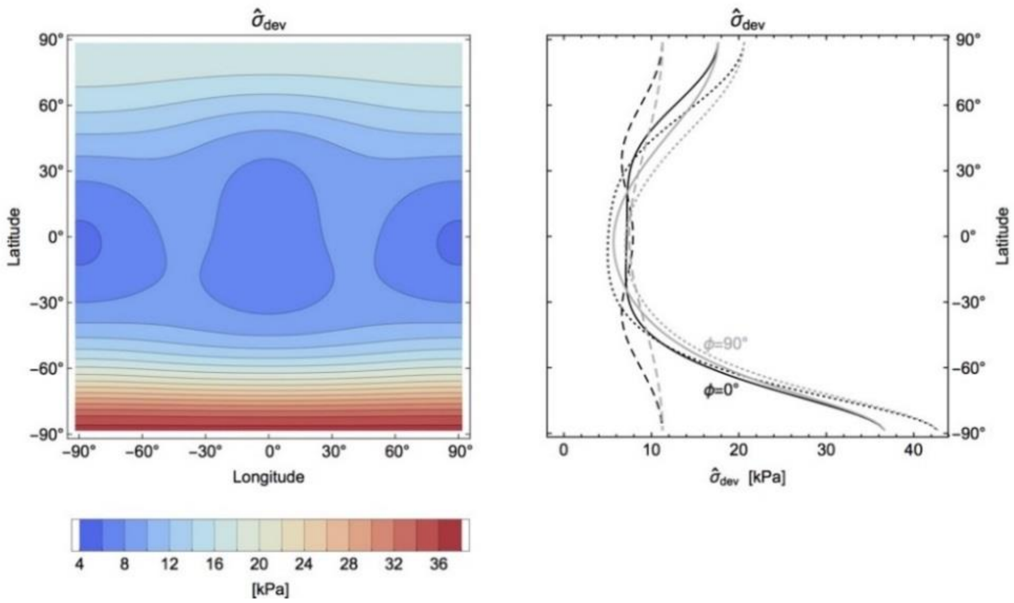

Average deviatoric stress at the surface of Enceladus due to tidal deformations. Left: stress magnitude in the Saturn-facing hemisphere. Right: meridional cross-sections of the surface stress at longitudes 0 and 90 degrees (solid curves), compared to the predictions for a crust of uniform thickness (dashed curves). Dotted curves show the predictions of membrane theory for a crust of variable thickness

If Enceladus's shell is conductive with isostatic thickness variations, crustal thinning at the poles strongly enhances the surface stress (stresses are approximately inversely proportional to the local shell thickness), while the surface deformation is only moderately enhanced at the south pole. For the shell structure deduced from libration and gravity/topography data, the amplification is about 60% at the north pole and about 3.3 at the south pole (see figure above). The combination of crustal thinning and convection below the poles could amplify south polar stresses by a factor of 10, explaining why geysers occur close to the south pole. It cannot account for the apparent time lag between the maximum plume brightness and the opening of tiger stripes, because viscoelastic effects are too weak to induce a sufficiently large delay. Besides demonstrating the role of crustal thinning and rheology softening in the localization of tectonic activity at the south pole of Enceladus, this new quantitative model has great prospects for developing realistic models of tidal dissipation within the crust.

In the frame of our work of habitability (5 years in Interuniversity Attraction Pole Planet TOPERS – Planets: Tracing the Transfer, Origin, Preservation, and Evolution of their ReservoirS)

Venus coupled evolution and consequences for magnetic field generation.

Venus lacks an internally generated magnetic field. Whether one existed in the past is unknown, but critical to atmospheric evolution and habitability. Canonical models assume the core of Venus has Earth-like structure and composition but cools too slowly to generate a magnetic dynamo. Core and mantle heat flow disappeared in these models after a transition in mantle dynamics associated with widespread volcanic resurfacing. However, recent studies of impact craters suggest more steady heat loss over geological time. MgO and/or SiO_2 precipitation from the core can also drive convection.

The Royal Observatory of Belgium developed a model coupling the mantle and the atmosphere with a planetary core simulation to study the range of parameters for core evolution. We modified a one-dimensional parameterization built for Earth on a fourth-order expansion of the radial density and gravity in the core. We re-evaluate the likelihood that Venus has an "Earth-like" core using numerical simulations of the coupled atmosphere-surface-mantle-core evolution.

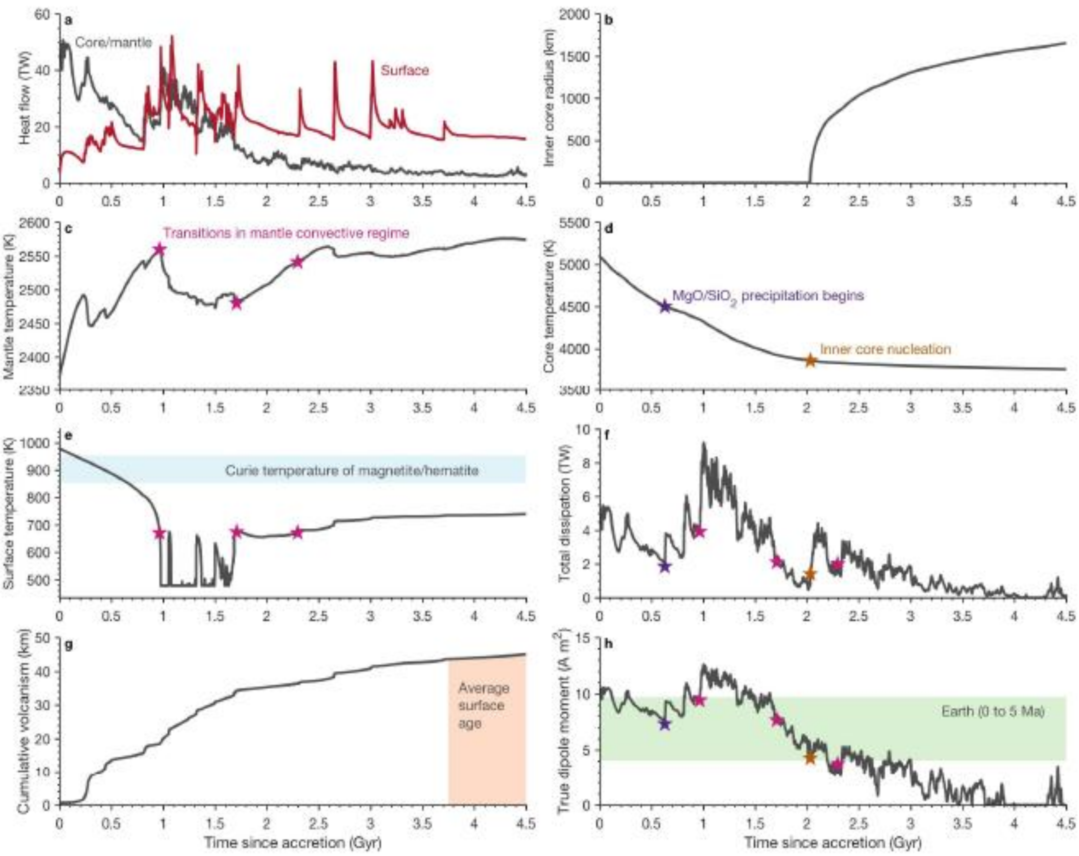

Evolution of Venus in our example simulation. (a) Core/mantle (black) and surface (red) heat flow. (b) Radius of the inner core. (c) Mean temperature in the mantle. Stars denote transitions in the regime of mantle convection from stagnant lid to mobile lid, and then gradually to stagnant lid again, followed by episodic lid until the present. (d) Temperature at the CMB. Stars indicate the temperatures at the onset of MgO and/or SiO2 precipitation and inner core nucleation. (e) Surface temperature. In blue, the range of Curie temperatures for magnetite and hematite. (f) Total dissipation produced in the core. (g) Melt production converted into an equivalent depth of volcanism on the surface. (h) Predicted TDM over time. The green, shaded region is the "1-sigma" range of paleointensities for Earth in the 0.05-5 Ma time interval

If the core actually contains more than 200 ppm of potassium [K], then our simulations indicate that a dynamo would probably exist today if no stratification were present. Concentrations in the range of 400-800 ppm are commonly invoked in models of Earth's evolution to prevent the inner core from growing larger than its present-day size while cooling remains fast enough at early times to sustain a dynamo. However, mineral physics experiments seem to favour [K] < 50-100 ppm for Earth's core based on the affinity of potassium for silicates instead of iron alloy. If the lowest estimates for thermal conductivity are confirmed, then the core of Venus must have completely solidified or preserved primordial compositional stratification. This scenario requires low (or even no) radiogenic heating in the core. Low initial temperatures are also required, and a cold core might form with compositional stratification anyways. On the other hand, higher conductivities are consistent with the conventional view that Venus has an “Earth-like" core that is cooling too slowly to have convection.

Characterization of water-rich exoplanets

This research addresses the characterization, modelling, thermal evolution and possible habitability of water-rich exoplanets. To model the evolution of water-rich planets (or moons) for arbitrary planet compositions, we used an interior structure model and 1D thermal evolution model developed at the Royal Observatory of Belgium. Both modules are included in the code CHIC (Coupling Habitability, Interior and Crust) of the Observatory. Using this code, we extended our study on investigating habitability limitation for water-rich planets of different compositions.

In order to classify the potential habitability of the water layer (possibly containing also high-pressure ice that can also melt from below), we use the following regime classification:

- Green: 100% O - a liquid ocean without high-pressure ice
- Yellow: 100% OIO - a liquid lower ocean (ocean-ice-ocean structure)
- Light orange: < 100% OIO - an ocean, liquid more than 50% of the time
- Dark orange: <50% OIO - an ocean liquid less than 50% of the time
- Red: 0% OIO - no lower ocean, the water layer always has an ocean-ice structure

We shown that planets smaller than Earth are more likely to be habitable (green area in the figure below) for Earth-like life than more massive planets. We furthermore looked into the detection methods for water in exoplanet atmospheres and future developments in space instruments, which would enable the detection of water on exoplanets.

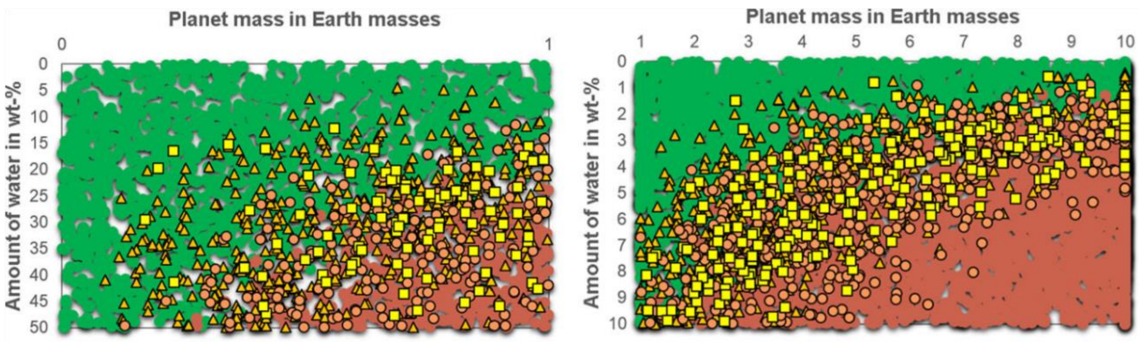

Possible habitability evaluation for planets of variable masses, compositions and interior parameters. The colours refer to liquid water layers (green), lower ocean layers (yellow), episodic lower ocean layers (orange) and high-pressure ice layers that are not molten at the bottom (red)

Clathrate, climate and habitability of Mars

Several detections of methane (CH_4) in the atmosphere of Mars have been reported from Earth-based and Mars orbiters as well as from in situ observations. Given the relatively short lifetime of CH_4 in the Martian atmosphere (standard photochemical models predict a lifetime of 300-600 terrestrial years), its presence implies the existence of a subsurface reservoir or an active primary source. CH_4 produced in the past or at present-day could be stored in subsurface reservoirs such as clathrate hydrates, which are crystalline compounds formed by the inclusion of gas molecules in the cavities of water molecules network. Thermodynamic conditions prevailing on Mars favour clathrate formation from near subsurface to deep down in the cryosphere. Their dissociation, initiated by a change in temperature, pressure or composition of the reservoir, is a possible mechanism for near-surface methane release on Mars. This work on clathrate hydrate stability and outgassing scenarios on Mars will provide valuable information and theoretical support for current and future space missions focusing on trace gases in the Martian atmosphere, especially the ESA satellite Trace Gas Orbiter.

To determine clathrate stability conditions, we followed a thermodynamic model based on statistical theory and on available experimental dissociation curves. This model has been coupled to a 1D thermal interior model to obtain clathrate stability zone variations in the subsurface of Mars as a function of pressure in pore spaces, thermal properties of the soil, local heat flow, fraction of CH_4 trapped in clathrates, as well as presence of perchlorates in the water involved in clathrate formation. We showed that the presence of magnesium perchlorate ($Mg(ClO_4)_2$) in the system, in addition to shifting the base of the hydrate stability zone, significantly affects its top at low latitudes. At the equator, CH_4 clathrates are stable deeper than 300 m in the presence of eutectic $Mg(ClO_4)_2$ brine and their stability zone has a thickness of a few hundred meters.

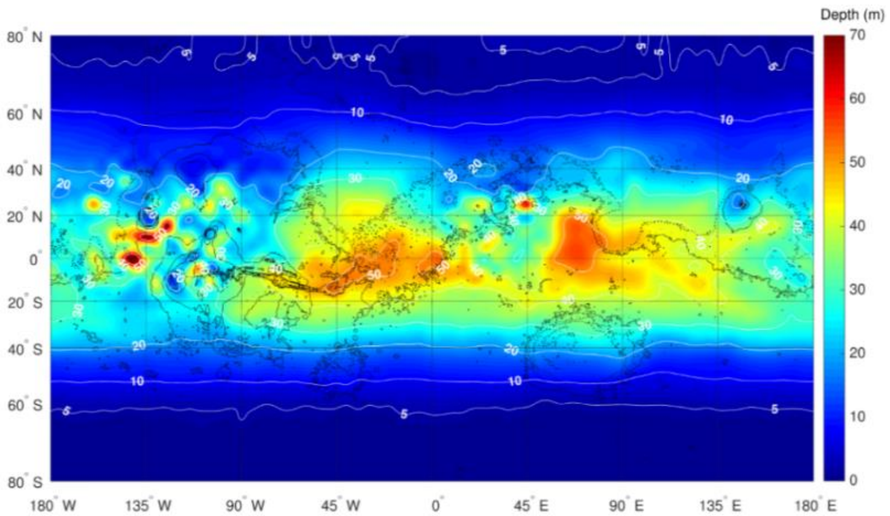

Depth (m) of the top of hydrate stability zone in present-day Martian subsurface for CH4-rich clathrates formed from a gas phase with 90% of methane

In a next step, the evolution with temperature of the methane fraction trapped in mixed CO_2-CH_4-N_2-Ar clathrate hydrates (structure I) from various initial compositions has been investigated. The relative abundance of CH_4 in clathrates slightly increases with the formation temperature and depends on the composition of the initial gas phase. When the abundance of methane in the initial gas phase is low, the fraction of trapped CH_4 is small and the clathrates contain mainly CO_2. On the contrary, when the initial gas phase is enriched in methane, the trapping of CH_4 is efficient. In addition, in the same initial concentration of methane and temperature conditions, the relative abundance of CH_4 is larger in clathrate hydrates formed from an initial gas phase richer in N_2.

Finally, present-day maps of CH_4-rich clathrate stability zone variations (see figure above) have been determined. Results show that CH_4-rich clathrates are stable in shallow subsurface with a stability zone strongly dependent on the average annual surface temperature and approaching the surface with increasing latitude.

Modelling of the interaction between the surface and the atmosphere

We modelled gas transport through porous Martian regolith (methane and water vapor transport) using a 1D diffusive model. We investigated several methane outgassing scenarios from clathrate hydrates and used the determined surface fluxes in the MarsWRF (modified version of the Weather Research and Forecasting model) and MRAMS (Mars Regional Atmospheric Modelling System) models to study methane transport in the Martian atmosphere. The results showed good match with observations depending on the emission location. At Gale Crater, simulations suggest that there must be a continuous release of methane to counteract atmospheric mixing, because the timescale of mixing is much shorter than the observed span of elevated methane levels. The water exchange between subsurface and atmosphere has been studied at *Mars Science Laboratory* and *Phoenix* landing sites as well as regions of trace gas observations.

Venus evolution in a multiple impacts Late Veneer scenarios

Late Veneer, at the end of accretion phase, could have been marked by impactors reaching sizes of up to 4000 km diameter and numbering between one and ten singular events. This series of events is especially critical for both light species and siderophile elements. ROB used stochastic simulations of impacts during this phase to investigate the effect of Late Veneer on the coupled atmosphere and mantle of Venus. Modelling of meteoritic erosion and replenishment for different impact histories was included. Large impacts affect mainly the mantle of Venus, while smaller and more numerous impacts affect primarily the atmosphere. Multiple impact scenarios are extremely chaotic.

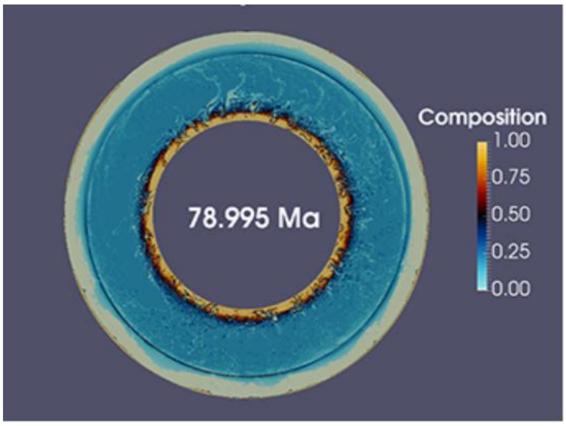

Mantle composition field of Venus after the reference succession of 9 reference impacts, illustrating upper mantle depletion

Subduction events that are directly caused by collisions were however observed. The upper mantle is widely mobilized and subjected to partial melting and displacement. A succession of random impacts of moderate sizes is more efficient (for the same cumulated mass) than a single event for depleting the upper mantle and causing widespread melting. Our scenarios show a thorough devolatilization of the upper mantle but leave the lower mantle relatively unaffected. Impacts increase surface temperature for millions to hundreds of million years, due to greenhouse effect. Mantle depletion, however, implies lower late evolution surface temperatures as degassing is hampered.

The effect of meteoritic impacts on the early Martian environment

There is now evidence that liquid water flowed on early Mars. Sophisticated climate modelling of ancient Mars assuming CO_2-dominated atmospheres have not yet been able to produce significant precipitations anywhere on the planet, unless reduced greenhouse gases (CH_4, H_2) are used. Warm and wet conditions could have been transient and produced in response to meteoritic impacts (valley networks formation and Late Heavy Bombardment both occurred 3.8 Gyr ago. We model the environmental effects of impacts to explore if they could trigger warm conditions.

In a first approach, we observe the surface heating by swarms of small impacts (radius < 10 km but numbering in the thousands and above) but neglected the role of the atmosphere. For each singular impact, eroding power, volatile content and energy input are all too low to cause long-term changes. However, they still heat up the surface of the planet for a limited time. The area and time where surface conditions are consistent with the presence of liquid water are computed. Results suggest that it is possible to heat up 20% of the surface of Mars during 50Myr, or 1% during the first 500 Myr, or at a later time, though the impactor flux becomes too small to sustain elevated temperatures.

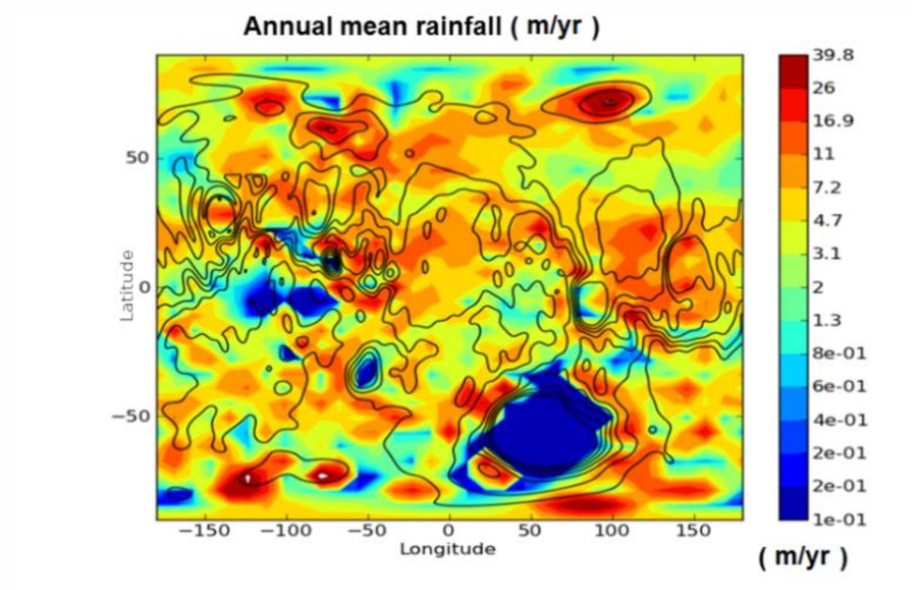

Annual mean rainfall rate following an impact event occurring on Early Mars (initially 1bar CO2-dominated atmosphere, obliquity of 45°)

In a second approach, we relied on a Martian Global Circulation Model to study the evolution of the atmosphere. We simulated the climatic effect of large meteoritic impactors (D>100km, N~10) hitting Mars at velocities ~10km/s. They initially force the atmosphere/surface and subsurface at temperatures up to 600 K, and vaporize up to several bars of water vapour. Results show that whatever the initial impact-induced temperatures and water vapour content injected, warm climates cannot be stable. It remains short-lived (~ 5-7 Martian years per bar of water vapour). A 100% thick cloud cover forms, producing rainfall, uniformly distributed on the planet. Warm and wet conditions that follow the largest impact events recorded on Mars should not only have been short-lived, but should also have produced precipitation patterns uniformly distributed on the planet, and thus uncorrelated with the position of the valley networks.

Seismology and Gravimetry

The main mission of the Operational Directorate "Seismology and Gravimetry" is studying variations of gravity and seismic activity, their causes and consequences. To support this scientific research and to provide the authorities, the media and the public with information about the seismic activity in real time in our region, this operational directorate develops and maintains a seismic network in Belgium.

Seismic activity

In 2017, 90 earthquakes occurred in a zone between 0° and 10°E longitude and 47° and 53°N latitude. The Royal Observatory of Belgium measured 5 induced events, 113 quarry blasts and 4 controlled explosions. The catalogue is complete for natural earthquakes and contains a selection of quarry blasts and earthquakes induced by human activities, e.g. linked to mass removal in open pit mines (see Figure below). In 2017, there were at least 4 measurable explosions at sea or close to the Belgian shore. Explosions are performed by the Belgian Army to destroy WW1 and WW2 bombs. 5 earthquakes and 3 induced events were felt in the region in 2017, but none in Belgium.

The felt earthquakes are mentioned in the Table below, with the total number of internet macroseismic inquiries received and mapped by the web portal ran by the ROB in collaboration with the University of Cologne. These events were felt by the local population who spontaneously answered the questionnaire.

Date and time of origin		Magnitude	Latitude	Longitude	Name	Inquiries
10/02/2017	20h24m UTC	ML 2.6	51.58	6.864	DINSLAKEN (DE)	3
14/03/2017	05h29m UTC	ML 2.5	50.34	7.442	OCHTENDUNG (DE)	16
23/03/2017	00h42m UTC	ML 2.4	51.07	6.825	DORMAGEN (DE)	1
30/03/2017	18h40m UTC	ML 2.1	50.39	7.389	PLAIDT (DE)	8
08/05/2017	03h18m UTC	ML 1.6	50.69	6.252	ROETGEN (DE)	4
14/06/2017	23h53m UTC	ML 2.6	50.35	7.186	KRUFT (DE)	26
08/11/2017	16h40m UTC	ML 2.8	50.87	6.866	HUERTH (DE)	59
19/12/2017	02h24m UTC	ML 1.7	50.97	6.655	BERGHEIM (DE)	10

Felt events in the region in 2017

The largest event recorded in the region in 2017 occurred on 8 November 2017 in Hürth (Germany, ML=2.8).

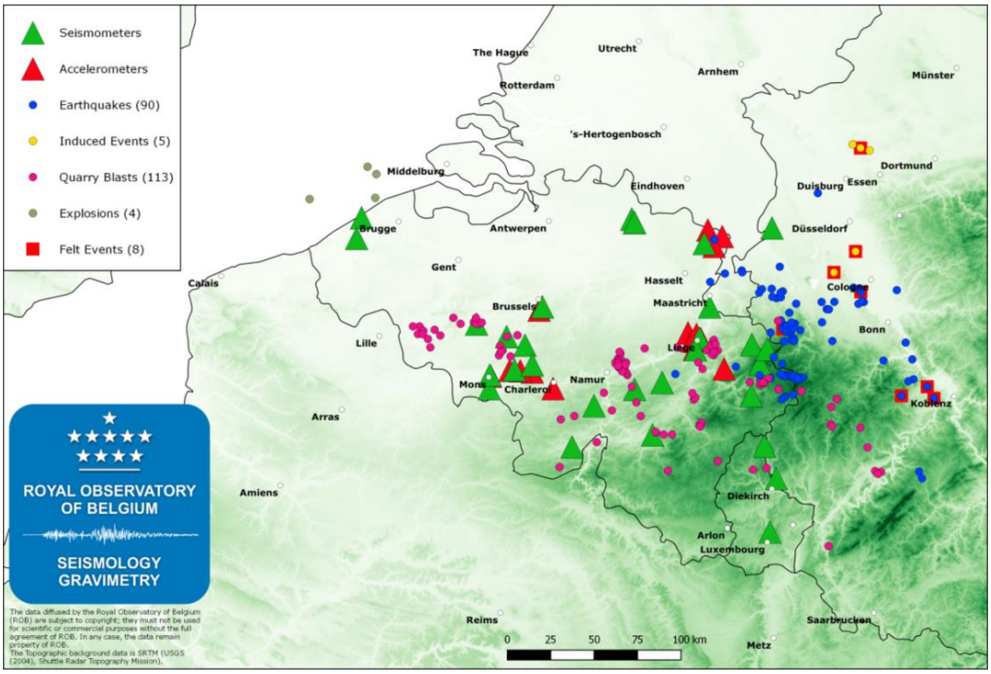

Events recorded in 2017 by the Belgian Seismic Network of the Royal Observatory of Belgium

For comparison, last year in 2016, 73 earthquakes occurred in and around Belgium. The largest was located in Növernich on 4 November 2016 (Germany, magnitude ML=2.8).

A Nineteenth-Century National Prussian Macroseismic Questionnaire

1700 handwritten pages of information on XIXth century earthquakes, this is the unexpected treasure discovered by scientists of the Royal Observatory of Belgium and the Cologne University in the record-office of Duisburg (Germany). The original documents covering the German, Belgian and Dutch border region include letters and most astonishingly formal macroseismic questionnaires of the Prussian authorities that have not been used in any modern scientific study to date. This discovery and the first results of their analysis were published in "Seismological Research Letters".

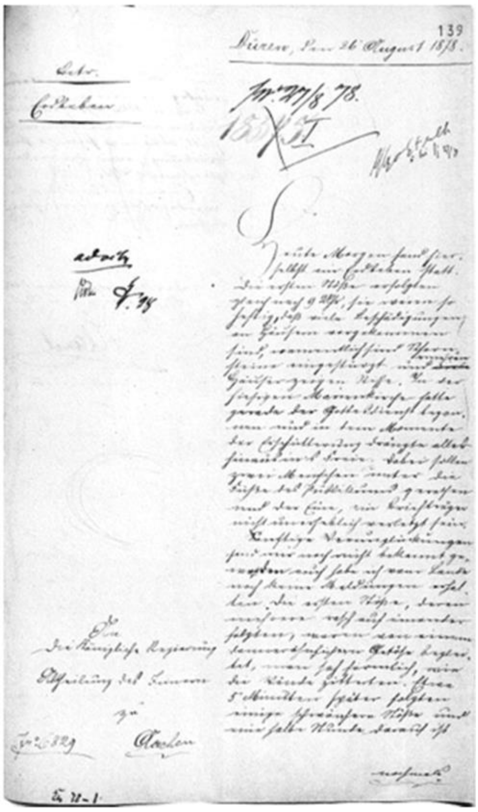

The two images report the questionnaire filled by the burgomaster of Niederzier and a letter describing macroseismic effects in Düren for the 26 August 1878 destructive earthquake

The complete analysis of the 1700 pages would certainly increase the knowledge about the XIXth century seismicity if funding were found to support the research. A better understanding of the effect of past earthquakes is fundamental to mitigate the societal, industrial and economic impact of future earthquakes.

A new application of a seismic method for monitoring underground water resources

The innovation: using seismic noise generated by oceans and which travel around the world to study tiny changes in seismic wave's velocity in aquifers. Decrease (or increase) of water resources stored in the underground is coupled with an increase (or decrease) of seismic wave velocities in the geological layers.

After three years of research, a team of scientists led by Dr T. Lecocq of the Royal Observatory of Belgium has identified a complementary method to existing hydrological monitoring techniques. To do so, the researchers have analysed 30 years of continuous seismic data: the longest seismic time series from a seismic network installed in southeast Germany in 1976 and that is still operational. The results show that it is possible to use seismic networks to study the state of the Earth crust at a scale previously out of reach. This scale fills the gap between existing local (piezometer or gravimeter) and regional (satellites) observations.

The team is composed of a hydrogeophysicist from the Université de Rennes, of seismologists from the Université Grenoble-Alpes, and from the German Federal Institute for Geosciences and Natural Resources.

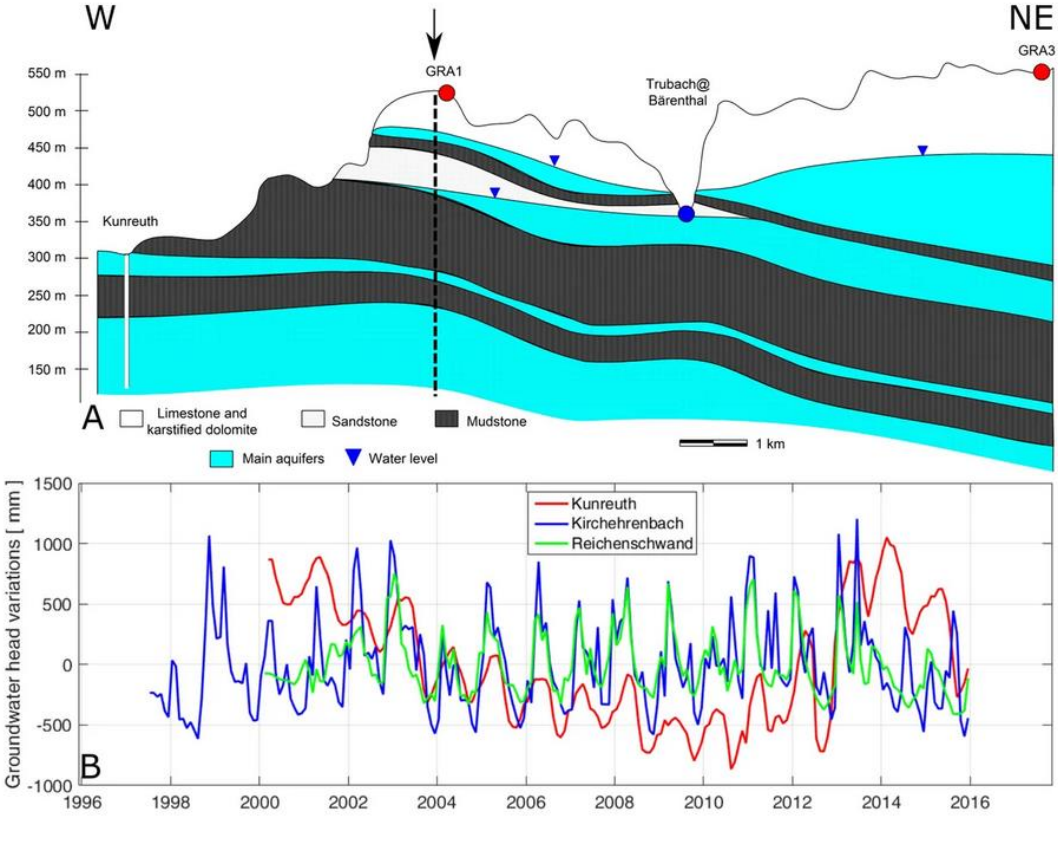

(A) Hydrogeological W-E cross-section (adapted from Krüger 199432) illustrating the complexity of the aquifers under the Gräfenberg array (stations GRA1 and GRA3 are shown), locations of example piezometric levels (triangles) and the Bärenthal discharge station (circle) in the area. The arrow indicates where the profile changes orientation (see Fig. 1). (B) Groundwater head variations for the three piezometers in the area (http://www.gkd.bayern.de): Kunreuth, Kirchehrenbach and Reichenschwand

Britain’s separation from mainland Europe

New evidence indicates that the opening of the Dover Strait — the narrowest gap between Britain and Europe — is the result of erosion caused by an overflowing glacial lake followed by catastrophic flooding. Determining how the Strait was breached has implications for our understanding of how the creation of island Britain altered colonization of the British Isles and changed the drainage of water from northwest Europe.

Artist’s impression of the land bridge connecting England and France before the formation of the Dover Strait. Water draining from a proglacial lake in the southern part of the North Sea spills over the land bridge through big waterfalls

During the ice ages, about 450,000 years ago, Britain was connected to continental Europe via a chalk ridge that extended from southeast England to northwest France. This land bridge acted like a huge dam behind which a proglacial lake formed. Previous theories have suggested that spillover from this glacial lake contributed to the opening of the Dover Strait, but testing this hypothesis has been limited by a lack of high-resolution data from the inferred breach-point.

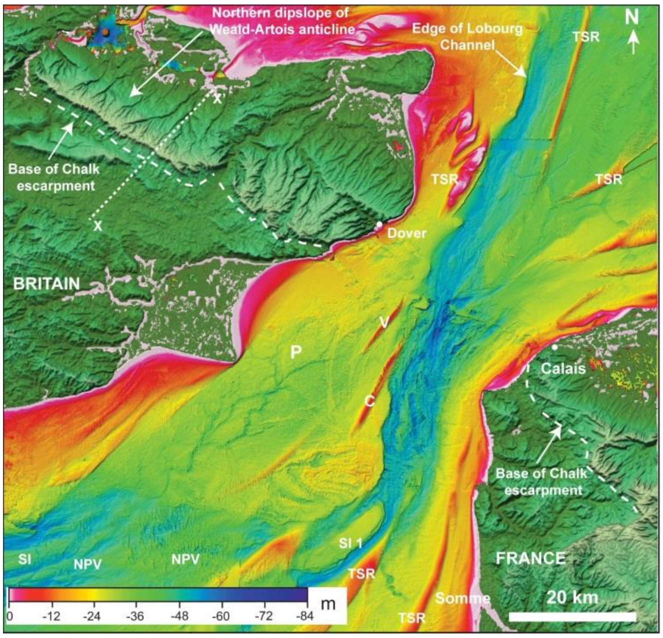

Bathymetric map of the Dover Strait, showing traces of the land bridge, eroded by a prominent valley in the central part of the Strait

In a study resulting from the cooperation of researchers from Imperial College, the Royal Observatory of Belgium, University of Gent and other international institutions, new evidence is presented indicating that the opening of the Strait involved at least two major episodes of erosion. The analyses support a model of lake overspill causing initial erosion around 450,000 years ago, through large waterfalls that eroded deep holes at the foot of the land bridge. In a second phase, the waterfalls cut through the chalk and caused the rock dam to fail, releasing huge volumes of water into the English Channel. The data reveals that this second catastrophic flooding event was needed to fully open the Dover Strait; the timing of this event is not clear, but it may have been around 160,000 years ago, the authors suggest.

This study is an unexpected outcome of the geophysical surveys that Royal Observatory of Belgium carried out in the Dover Strait onboard R/V Belgica in 2010 and 2012, with the objective to search for active faults that could have generated the historical 1580 earthquake (M=6). It also frames in the Ph.D. study of David Garcia-Moreno, which was initiated at the Observatory, and finalized this year at the Ghent University.

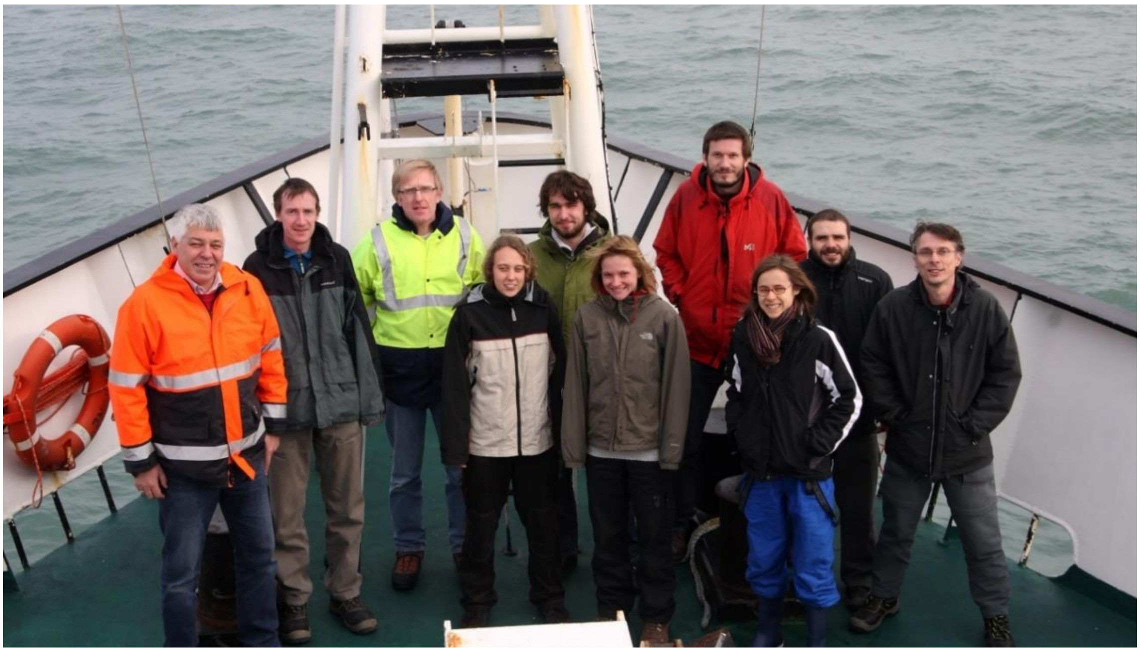

Scientific crew (including three researchers of the Observatory) of the Belgica survey 2012/03 in the Dover Strait, during which part of the data used in the study was collected

Reviews of geophysics

The Operational Directorate “Seismology and Gravimetry” led a paper published in the prestigious *Reviews of Geophysics*, the AGU journal that provides overviews and syntheses of recent research in all areas of the Earth and space sciences. This illustrates the long tradition of the Royal Observatory of Belgium in terms of gravity measurements.

Why measuring gravity? Factors such as fluctuations in Earth’s rotation and tides, changes in ground water content, underground movements of magma, or vertical land movements mean that gravity changes over time.

Hence, monitoring changes in gravity over time provides information on deformations of the solid Earth and changes in the distribution of mass. This can be related to their geophysical causes such as tectonic and volcanic activity, past and present ice-mass changes, tides and the dynamics of the oceans or aquifers. For example, gravimetry has proven useful on volcanoes, where combining gravity and deformation measurements has permitted discrimination between gas, water and magma intrusion, assessing voids opening or magma density changes associated with degassing.

Today’s gravimeters can achieve a high level of accuracy: a superconducting gravimeter can detect the gravitational effect of a child sitting one meter above the instrument. This is the equivalent of one millimeter in the ground water content.

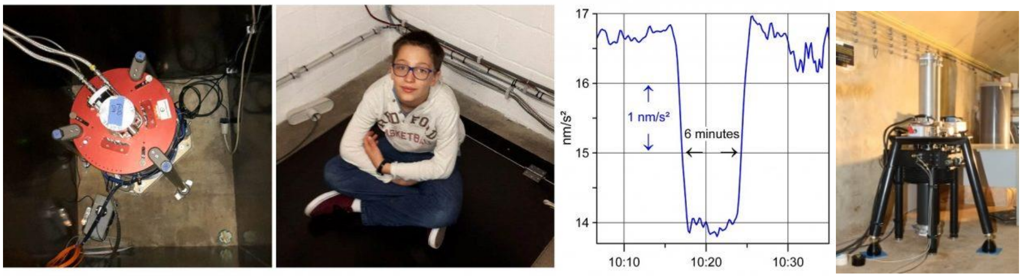

Left: The relative superconducting gravimeter installed in a shaft at the Rochefort station, Belgium. Center-left: A 13-year old boy, weighing 45 kilograms, sat with his navel 1 meter above the instrument. Center-Right: The gravitational effect of the boy sitting for 6 minutes: his mass induced a decrease in gravity of 0.28 billionth of g. Right: the FG5 absolute gravimeter measuring at the Membach station

Another paper was published in *EOS*, reporting on double world record set in September 2017 by the superconducting gravimeter located at the Membach station. The records are for the longest continuous time spent measuring gravity variations using a single superconducting gravimeter in the same place, as well as the longest superconducting levitation of an artifact. On 18 September 2017, this instrument had monitored gravity changes continuously for 8,081 days—22 years and 45 days and still participate in numerous scientific projects.

Astronomy and Astrophysics

The astronomers of the Operational Directorate "Astronomy and Astrophysics" do research in astronomy and they also observe solar system objects. Stellar evolution, mass loss of stars, variable and multiple stars as well as rapidly rotating stars are studied. Astrometry of minor planets is carried out and planetary satellites are observed. The researchers are active in the preparation and/or reduction and interpretation of data coming from dedicated observational campaigns, large scale surveys and space telescopes.
The service maintains databases and provides software for scientists. General information on astronomical and related phenomena are given to the public and to the press. Digitisation and archiving of photographic plates is also a task of this group.

The variable millimetre emission of Cyg OB2 #8A

Cyg OB2 #8A consists of two very massive and luminous stars that orbit each other with a period of 21.9 days. The luminosity of these stars is so high that it blows away their outer layers, forming a stellar wind. Because the two stars are close to each other, their winds collide. This wind-wind collision heats the material, leading to additional emission, and accelerates some of the electrons to relativistic speeds, thereby generating synchrotron emission. This synchrotron emission is most easily detected at centimetre radio wavelengths. The centimetre radio fluxes go up and down as the distance between the two stars in their eccentric orbit changes, because the strength of the wind-wind collision changes.

A theoretical prediction claims that, at shorter wavelengths (millimetre rather than centimetre), we would start seeing more radiation from the heated material rather than from the accelerated electrons. To verify this prediction, a team from the Royal Observatory of Belgium and University College London observed Cyg OB2 #8A at a wavelength of 3 mm with the NOrthern Extended Millimeter Array (NOEMA – figure on the right), an interferometer array which combines the observations of a number of telescopes, so that a higher-resolution image can be obtained.

The NOEMA array of millimetre telescopes, located in the French Alps. Photo credit: IRAM

The collaboration, led by Dr R. Blomme of the Royal Observatory of Belgium, also managed to detect its visual companion, Cyg OB2 #8B (see figure below on the left). This is also a very massive and luminous star, and we were able to determine its mass-loss rate due to its stellar wind.

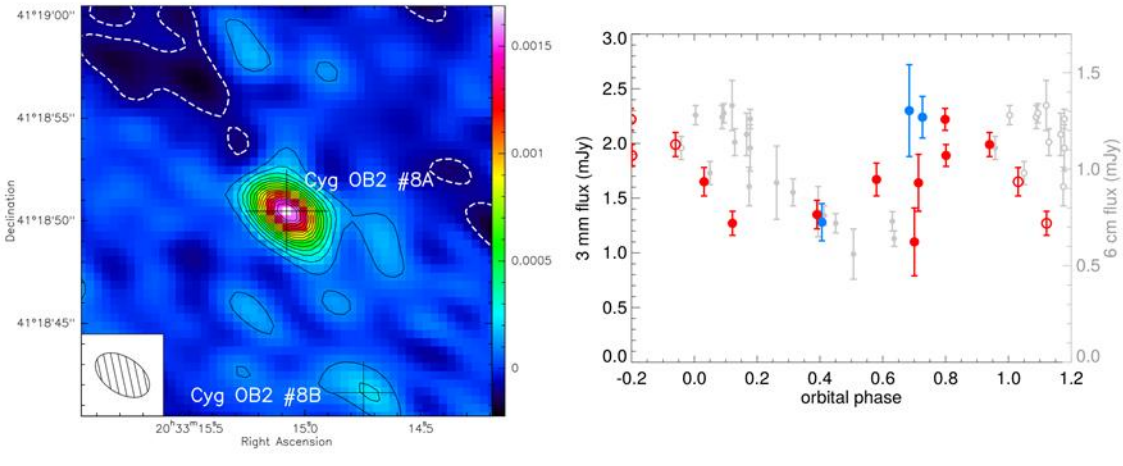

The map of the 3-mm emission around Cyg OB2 #8A (left) and the variation of its 3-mm fluxes as a function of orbital phase (right). The grey data show the 6-cm radio fluxes

When we plot the Cyg OB2 #8A 3-mm fluxes as a function of the phase in the orbit of this binary system (see figure above on the right), we see that they also go up and down with the orbital phase, just like the 6-cm radio fluxes. We then used theoretical models to see whether we could explain this behaviour of the 3-mm emission. The conclusion of this modelling is that, most likely, both the heated material and the synchrotron emission contribute to the 3-mm emission.

U Ant: Ageing Star Blows Off Smoky Bubble

U Antliae is a carbon star, i.e. an evolved, cool and luminous star of the Asymptotic Giant Branch type, at a distance of about 850 light years. Around 2700 years ago, U Antliae went through a short period of very intense mass loss. During this period of only a few hundred years, the material making up the shell (see figure below on the left) was ejected at high speed. Examination of this shell also shows some evidence of thin, wispy gas clouds known as filamentary substructures. To put things in perspective, the shell is 100 times larger than the Solar System.

This spectacular view was made possible by the unique ability to create sharp images at multiple wavelengths that is provided by the ALMA (Atacama Large Millimeter/submillimeter Array) radio telescope, located in the Atacama Desert in Chile. ALMA can see much finer structure in the U Antliae shell than has previously been possible.

The new ALMA data are not just a single image; ALMA produces a three-dimensional dataset (a data cube) with each slice being observed at a slightly different wavelength. Because of the Doppler Effect, this means that different slices of the data cube show images of gas moving at different speeds towards or away from the observer at Earth. By displaying the different velocities the astronomers of this project, in which participated Dr M. Groenewegen of the Royal Observatory of Belgium, can cut this cosmic bubble into virtual slices just as we do in computer tomography of a human body. This is shown in the second ALMA image (see figure below on the right).

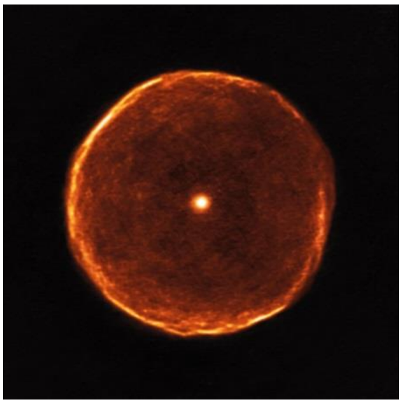

First ALMA image

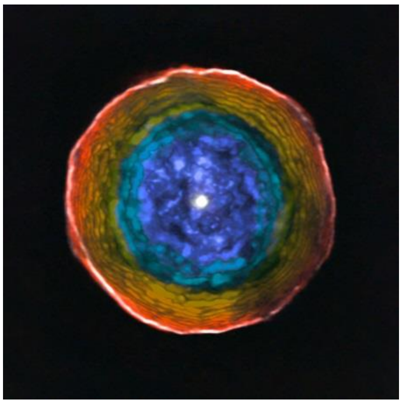

Second ALMA image

The colors show the motion of the glowing material in the shell along the line of sight to the Earth. Blue material lies between us and the central star, and is moving towards us. Red material around the edge is moving away from the star, but not towards the Earth.

Understanding the chemical composition of the shells and atmospheres of these stars, and how these shells form by mass loss, is important to properly understand how stars evolve in the early Universe and also how galaxies evolved. Shells such as the one around U Antliae show a rich variety of chemical compounds based on carbon and other elements. They also help to recycle matter, and contribute up to 70% of the dust between the stars.

The photoionization code Cloudy

Galaxies contain many stars. Our own Milky Way galaxy may have roughly 250 billion stars. Despite this very large number, galaxies appear to consist mostly of empty space. However, there is a very tenuous mix of gas and dust between the stars: the interstellar medium (ISM). The density of this material is extremely low: between one particle per cm^3 in the general ISM and 10,000 to 1,000,000 particles per cm^3 in "dense" regions. In most of the ISM, the density is lower than the hardest vacuum ever created in laboratories on Earth. Still, we can observe and study the ISM because there are vast regions of space filled with it, leading to a significant cumulative effect.

"The pillars of creation" is a star forming region in the Eagle Nebula. In the dark regions, new stars are being formed. The ultraviolet light coming from recently formed stars that evaporated the part of the cloud that surrounds them is eroding the nebula. Credit: NASA

The ISM is a mix of primordial and processed material. The primordial material was a direct product of the Big Bang and consists almost exclusively of hydrogen and helium. The galaxy and the first generation of stars were formed out of this material. The processed material consists of heavier elements (carbon, oxygen…) produced by nuclear reactions occurring inside stars during the final stages of their evolution. These nuclear reaction products are eventually expelled into the ISM. In this mix of material, dense regions form, called molecular clouds, where new stars can be born (see an example in the figure above). This second generation of stars contains hydrogen and helium, but also heavier elements created by the first generation of stars. We have this way a cyclic process where stars are formed out of the ISM, create heavier elements, expel that material back into the ISM which will be used to form new stars. Each turn of this cycle create heavier and heavier elements.

The ISM plays an important role in the evolution of a galaxy as it creates the molecular clouds in which new stars and planetary systems are formed. Moreover, since they are dense, molecular clouds shield the inner regions from ultraviolet light emitted by other stars, allowing chemical reactions to take place, and ice mantles to grow on dust particles. These ice mantles are well suited to allow complex organic molecules, such as pre-biotic molecules, to form. Hence, molecular clouds may play a role in the creation of life. Given their importance, molecular clouds and star forming regions are widely studied.

Stars that are close to the end of their life eject a lot of gas and dust into the ISM, forming a circumstellar shell around the central star. As the central star evolves and heats up, it will ionize the gas in the circumstellar shell allowing it to shine in colours. The figure below shows an example, which is a false-colour composite of ultraviolet and infrared images of the Helix nebula. Such objects are ideal laboratories as the material in the circumstellar shell exclusively comes from a single star, making the interpretation of observations easier. They can notably be used to test evolutionary models and study mass loss processes, dust formation, molecular chemistry and nuclear reactions.

The Helix nebula (NGC 7293) is one of the best known examples of a highly evolved planetary nebula. Near the center many high-density globules are visible. Credit: NASA

In order to interpret observations of the ISM, researchers need a modelling code that allows them to derive physical quantities such as gas temperature and density, chemical composition, and the degree of ionization, as well as properties of the source of light (often a star). For this purpose, an international team, including Dr P. van Hoof of the Royal Observatory of Belgium, developed the open source photoionization code Cloudy (https://nublado.org/). The aim of the code is to model the ISM in the widest possible sense, with emphasis on the detailed treatment of physical processes. As the name indicates, it can handle regions that are ionized by photons, but it can also model regions that are heated solely by collisions as well as neutral and molecular regions. To our knowledge, the code Cloudyy is the only one that can treat all these processes in a self-consistent way.

The code Cloudy is widely used and was cited each year by more than 300 scientific papers. ASTRONET named it in its 2008 report as one of the "power-horses" in the section "public software for theory". A code like Cloudy needs continuous development to update the physics and include new fundamental data. In 2017, a new version called c17.00 was released. This is the first major release in 4 years. It contains many major improvements, such as an upgrade of the atomic line database and a new option to run grids of models in parallel. The code is about two times faster than the previous version.

The Belgian Repository of fundamental Atomic Data and Stellar Spectra (BRASS)

Accurate atomic line transition data are fundamental input parameters in astrophysics. Uncertainties and errors in adopted fundamental atomic data may systematically propagate throughout all fields of astrophysics, from star formation to galactic evolution. It is very difficult to obtain accurate fundamental atomic data of astrophysical interest from laboratory measurements. Only a limited number of repositories offer these values. The atomic repositories are often complementary rather than redundant, and can provide incomplete or inaccurate information. Important quality assessments of the provided atomic data values are scarce, which very much complicates the validation of results that follow from their application.

The BRASS Spectra Data Interface showing online interactive plots of the benchmark spectra of the Sun and 51 Peg with spectral line identifications and fundamental atomic data

The Belgian Repository of fundamental Atomic Data and Stellar Spectra - BRASS project takes a first, although crucial, step towards removing all systematic errors in atomic input data required for quantitative stellar spectroscopy. BRASS thoroughly assesses the quality of fundamental atomic data available in the largest repositories by comparing very high-quality observed stellar spectra with state-of-the-art theoretical spectra. Whereas this type of study has currently been carried out for very few stars at the time, and mostly limited to comparable spectral types assembled from various sources, BRASS combines, analyses, and offers the community the first uniform large collection of benchmark and reference stars (see figure above). This study will be more complete than any other to date in terms of coverage of the stellar parameter space, as well as the spectral wavelength coverage.

The BRASS project combines the scientific know-how of several national and international research teams in quantitative stellar spectroscopy, including the Royal Observatory of Belgium (ROB), the University of Leuven (KUL), the European Southern Observatory (ESO/Paranal), Chile, and the Université Libre de Bruxelles (ULB). It also involves the University of Antwerp (UA) and the Vereniging voor Sterrenkunde (VVS) in the networking project. BRASS gathers expertise required for addressing various aspects of observational and theoretical astrophysics, atomic physics, and software development. To achieve these goals, the project uses a large sample of stellar spectra collected from Belgian (Mercator-HERMES) and European (ESO-VLT-UVES) observation facilities over the last two decades. The datasets will be accessible to the scientific community. More information about the project, its data interface and science publications is available at: http://brass.sdf.org.

Solar Physics and Space Weather

The Operational Directorate "Solar Physics and Space Weather" studies the outer layers and the atmosphere of the Sun, with a particular focus on solar activity and the influence it exerts on the Earth and its space environment (space weather).

Extreme Ultraviolet Imager (EUI) ready for launch!

EUI delivery, integration & press conference

On June 9, 2017, the solar telescope EUI was delivered to Airbus UK. Integration of EUI onto the Solar Orbiter satellite was completed at Airbus on September 5, 2017. In view of the readiness of EUI for launch and the prospect of its exciting journey ahead, the Royal Observatory of Belgium and the Centre Spatial de Liège (CSL) organized a joint press conference in Liège on June 2, 2017.

Members of the EUI team (ROB &CSL) in front of the instrument at the occasion of the press conference on June 2

EUI was built by an international consortium under the leadership of a dedicated team at the Centre Spatial de Liège. After launch, the Royal Observatory of Belgium will operate the instrument. All of this is possible thanks to the generous support from BELSPO through ESA/PRODEX.

The Solar Orbiter mission

In sci-fi movies, spacecraft travel to the stars. With the "Solar Orbiter" spacecraft, mankind will make a small step towards the stars and travel first to its own star: the Sun. Obviously, Solar Orbiter will need special protection, the so-called heat shield, to withstand the enormous heat when travelling inward beyond the closest planet, Mercury. Solar Orbiter will not only observe the Sun from closer by than ever: its orbit will also allow us to see the backside and the poles, which are hard to observe from Earth's perspective.

Solar Orbiter is an ESA-led mission with strong NASA participation. Its launch is planned in 2020, and it will initiate a few rounds of planetary snooker. Two close encounters to Venus will alter the spacecraft's orbit, sending it to a close rendezvous with Earth, which will bring it close to Venus once again. After a last gravitational slingshot from Venus, the desired orbit will be reached. Science operations will run from 2023 until 2026, and the mission may be extended afterwards till 2029.

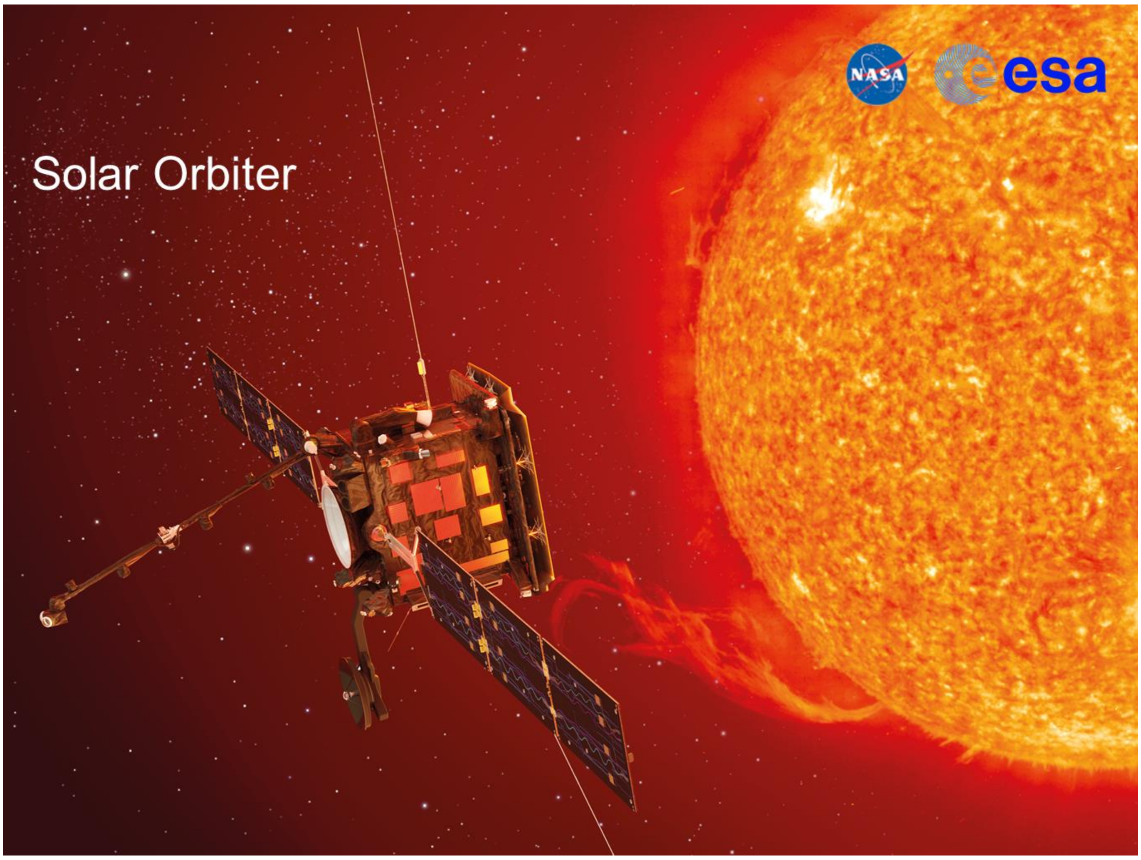

The Solar Orbiter spacecraft approaching the Sun, to more than 3 times closer to the Sun than the Earth

On board Solar Orbiter, ten instruments will investigate the Sun and the local environment of the spacecraft. In-situ instruments will monitor the solar wind, magnetic fields and energetic particles in the vicinity of the spacecraft, while remote-sensing instruments will take a fast succession of high resolution pictures from the Sun in several wavelengths.

The resulting combination of instruments, combined with the unique orbit, distinguishes Solar Orbiter from all previous and current missions, enabling science which can be achieved in no other way. Solar Orbiter can therefore be seen as a next step in our exploration of the Sun and the Solar System.

The EUI telescope onboard Solar Orbiter

The "Extreme Ultraviolet Imager" (EUI), one of the prime instruments on board Solar Orbiter, is a bundle of 3 telescopes for observations of the solar upper atmosphere, at unprecedented spatial resolution and with a large-angle view to see the full Sun, even from close by.

EUI will let us identify features on the Sun that are only 200 km apart, which is 5 times sharper than major contemporary missions such as NASA's SDO (Solar Dynamics Observatory) mission. The large-angle view is needed to link structures and dynamic phenomena observed in high-resolution on the solar disc with the in-situ observations made by other instruments in the solar wind plasma surrounding the spacecraft.

Observing in extreme ultraviolet, EUI is perfectly placed to observe magnetic loops through which solar plasma is suspended far above the solar surface. These magnetic loops are very dynamic and can suddenly brighten and even burst. If these eruptions are directed towards Earth, they can have severe consequences on our technology such as GPS and radio communication, power grids, and pipelines.

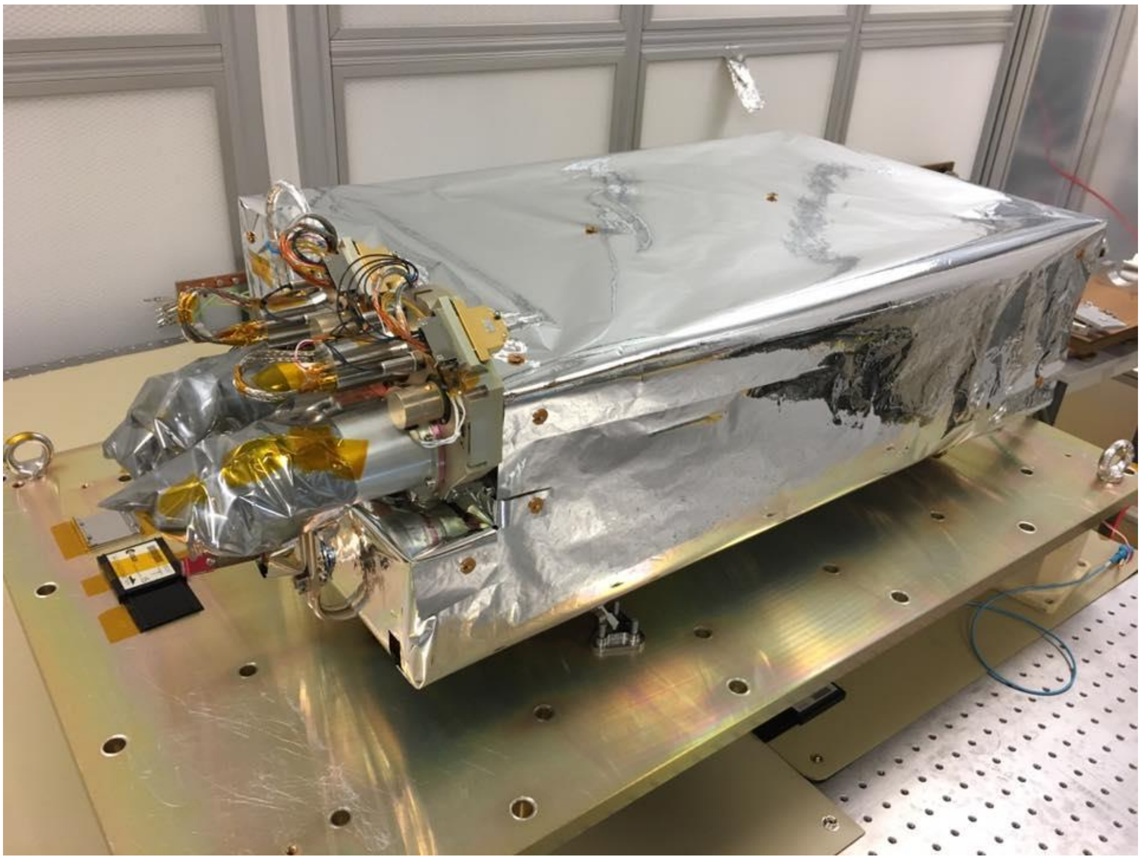

The EUI telescopes just before delivery to Airbus, June 2017

Because of its close approach, EUI will be able to make exceptionally detailed images of our star. These will help scientists to unlock the secrets of the solar atmosphere.

Contribution to an international campaign of observations of the Sun – Opportunity to test a “lucky imaging” technique

From 27 March 2017 to 04 April 2017, the Royal Observatory of Belgium took part in the international campaign “Joint observations of disk and off-disk structures between IRIS, HINODE, SUMER/SOHO and GBOs”[1] (HOP 334), which coordinated the observations of about twenty space-based and ground-based observatories aiming at the Sun. This campaign was primarily meant to support what is likely the last run of observations with the FUV-VUV spectrometer SUMER on-board SOHO, one of the rare instruments capable of observing the Lyman α spectral profile with high wavelength resolution.

The campaign had various targets: active regions (especially when they erupt), sunspots, filaments/prominences, spicules or coronal rain, observed over a wide range of wavelengths to cover different regimes of temperature and emission processes, for a comprehensive observation of the solar atmosphere from the photosphere to the extended corona.

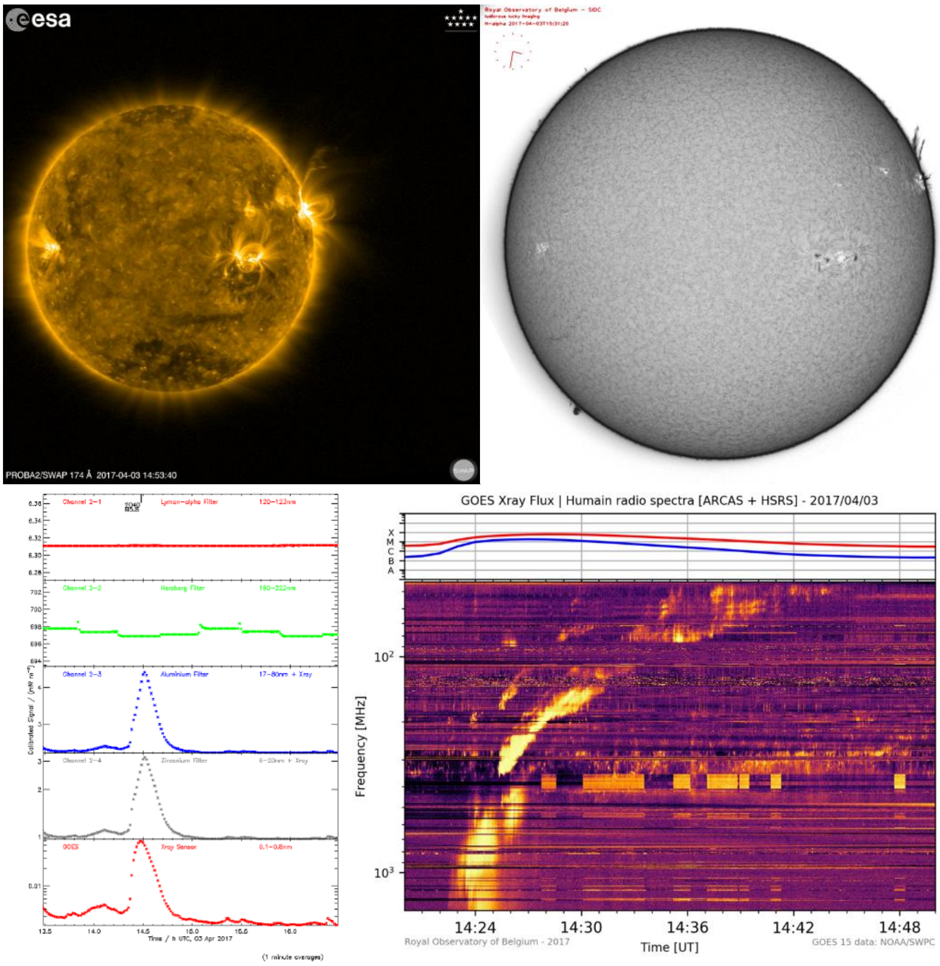

Observations with instruments of the Royal Observatory of Belgium during a solar eruption on April 3rd, 2017. From top to bottom and from right to left: PROBA2/SWAP off-pointed image; USET/ Hα image; light curves in the 4 different channels of PROBA2/LYRA; radio observations at the Humain station. (The GOES X-ray light curves are also shown for indication)

[1] http://www.isas.jaxa.jp/home/solar/hinode_op/hop.php?hop=0334

The Royal Observatory of Belgium contributed with two instruments on board the PROBA2 spacecraft. The first one is the SWAP imager, which observes the Sun at 17.4 nm (EUV) and performs off-pointing manoeuvers to follow erupting material further away than usual from the surface, and with an increased cadence. The second one is the LYRA radiometer, which observed the Sun with channels recording soft X rays, EUV, Herzberg continuum and Lyman α. The Observatory also contributed with ground-based telescopes. The radiospectrographs of the Humain station (Callisto, ARCAS and HSRS) covered the range 45-1495 MHz to detect energetic electrons travelling through the corona and possibly into the interplanetary medium. Three USET visible telescopes in Uccle observed with Hα, Ca II k and broadband “white light” filters.

During the campaign, about 10 noticeable radio events and 2 M-class flares were observed by the instruments of the Royal Observatory of Belgium, one of the flares even producing a substantial signal in the Lyman α channel of LYRA. This results in a unique data set associating space-borne instruments and ground-based observatories all over the world with complementary time coverage, “seeing” conditions and wavelength coverage, from the radio to X-ray wavelengths ranges.

Lucky imaging

The HOP 334 campaign appeared as an opportunity to test the “lucky imaging” technique on the Hα and Ca II k channels of the USET telescopes in Uccle. The idea of lucky imaging is to combine (parts of) the best images - recorded within a short time interval - into a single one, to reduce the distortion by the atmospheric turbulence and increase the signal-to-noise ratio. This allows us to see more and fainter details on the Sun. The camera software was modified to record images at its maximum cadence of almost four images per second, and an optimal effective cadence of 10 s was chosen to match the cadence of other instruments taking part in the campaign. This cadence of 10 seconds makes it possible to observe dynamic phenomena in the chromosphere, especially during eruptions.

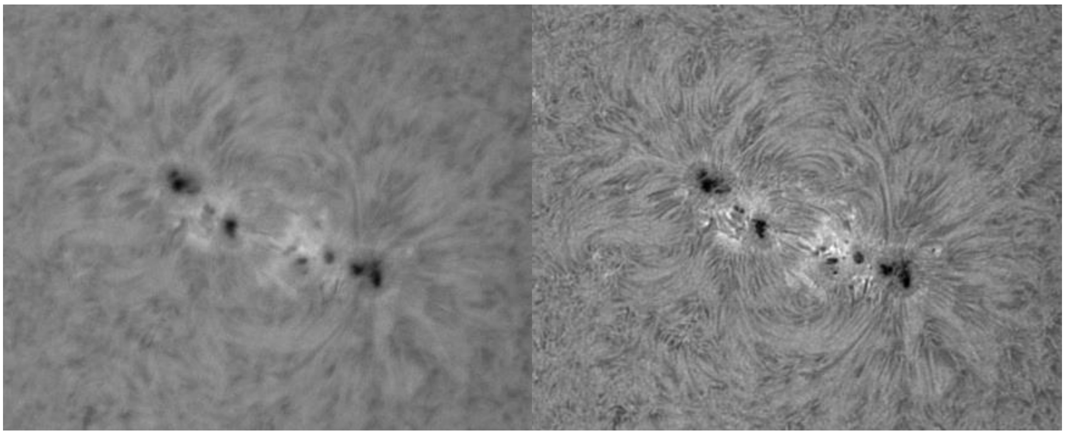

On the left a close-up of active region AR 12645 imaged on April 2, 2017 at 08:00UTC image with the USET Hα telescope. On the right the same region with much improved details as a result of “lucky imaging” applied to 10 seconds worth of images

Because a full day of observations in these conditions produces hundreds of Gigabytes (8 TB in total for the complete campaign!), it was not possible to store them all on the acquisition computers of USET. A special organisation was needed to cope with this large data flux, and the processing of the data - including calibration corrections - is also challenging. This campaign paved the way for more regular high cadence observations of this type, to produce high cadence and high quality images of dynamic events occurring in the solar chromosphere.

Signatures of a not so typical solar eruption

On August 14, 2010, a wide-angled coronal mass ejection (CME) was observed. This solar eruption originated from a destabilized filament (a bundle of twisted magnetic field lines that holds solar plasma) which connected two active regions. The unwinding of this filament gave the eruption an untwisting motion that drew the attention of many observers. The different stages of the eruption are shown in the figure below.

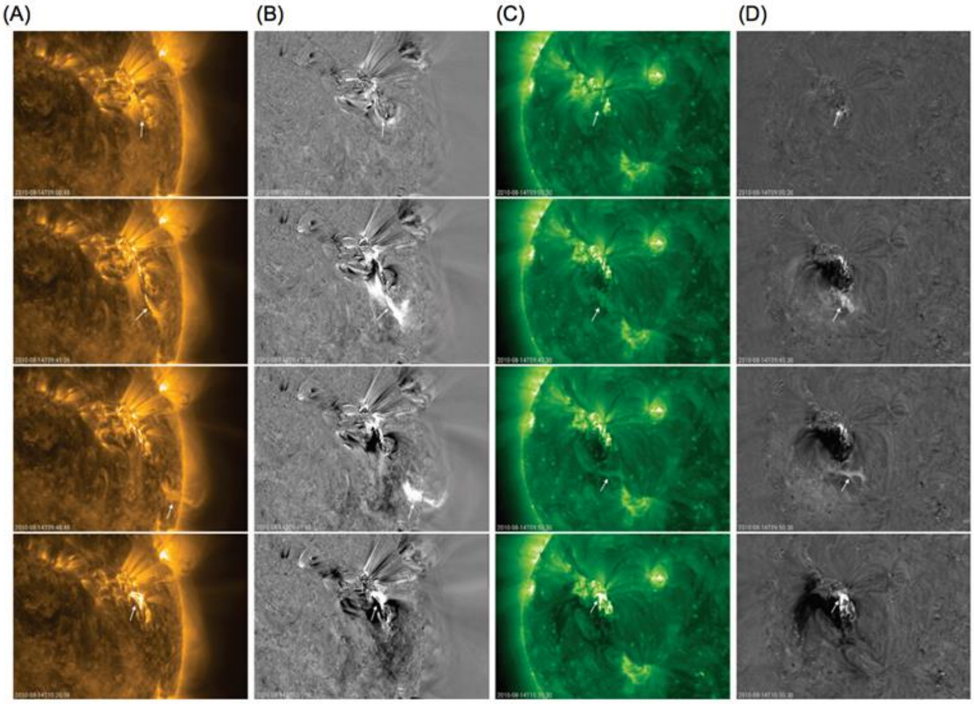

SDO/AIA 171 Å plain and base difference images (A, B) of the eruption on August 14, 2010, combined with STEREO-A EUVI 195 Å images (plain and base difference, C, D) taken at approximately the same time. These images show (from top to bottom and indicated by the white arrows): the rising filament, its unwinding motion as it is hurled into space, and the post-eruptive loops

In addition to the erupting filament and the associated CME, several other low-coronal signatures that typically indicate the occurrence of a solar eruption were associated with this event. Solar observers, acting on information obtained from both satellites and ground-based stations, also reported on a solar flare, radio bursts, a EUV darkening, and a proton event.

However, what was striking is that this CME was a very fast one (with a velocity above 900 km/s), while the accompanying solar flare was quite weak (C4.4, where 'C' stands for a common flare). This is not what is expected from the proposed solar eruption models: most often strong solar flares and fast CMEs go hand in hand.

To investigate what was then different in this case, we analysed the initiation and the trajectory of the associated CME using three-dimensional reconstruction techniques. The resulting diagram of the height of the CME flux rope as it rises up in time is shown in the figure below. For this plot, measurements were made on images taken by different EUV telescopes as well as coronagraphs. Note especially how the unique large field-of-view of the SWAP EUV telescope onboard the PROBA2 ESA spacecraft is able to fill the observational gap between the other EUV telescopes and the coronagraphs. SWAP's observations were especially useful to measure the strong acceleration that the CME flux rope undergoes at this height during the eruption.

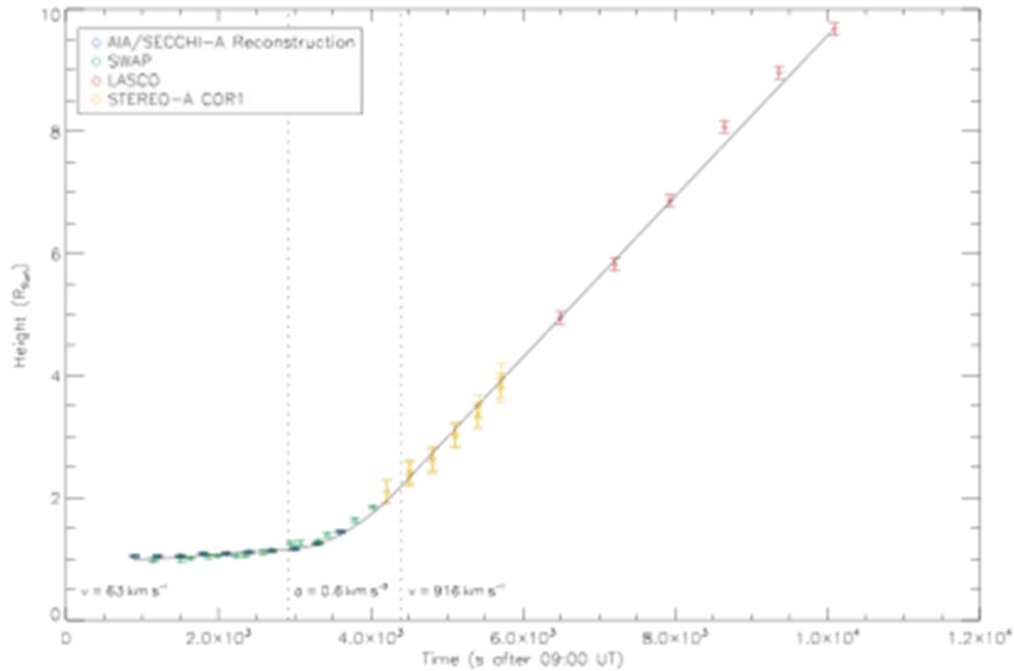

Height-time diagram for the CME on August 14, 2010, combining measurements made using observations by different EUV imagers and coronagraphs

Our detailed analysis of the August 14 CME led to the conclusion that this eruption was most likely triggered by an ideal MHD instability. As a result, the eruption was not associated with significant magnetic reconnection, which explains the occurrence of only a weak flare in association with a very powerful CME.

Had this solar eruption occurred just a few days earlier, it could have been a significant event for space weather, as the CME would have been directed towards the Earth. The risk of underestimating the strength of this eruption based solely on the C4.4 flare illustrates the need to include all eruption signatures in event analyses in order to obtain a complete picture of a solar eruption and assess its possible space weather impact.

The November 4th 2015 event

Solar flares and other eruptive events are often accompanied by bursts of radio emission produced by energetic electrons. The spectral signature of these bursts provides solar physicists an insight on the scenario of the eruptive event taking place. The underlying physics giving rise to the radio emission makes the intensity of these bursts essentially unrelated with the energy of the associated electrons, which means for example that tiny eruptive events, not detectable in EUV of soft Xray, can easily be observed in radio. On the other extreme, if strong flares are often associated with radio bursts, the intensity of the latter does not with the strength of the flare.

This wide range of burst magnitude requires tools that are extremely sensitive, and solar radio astronomers, like all radio astronomers, are very wary in protecting their observations from interferences produced by other users of the radio spectrum. On some occasions, however, "Mother Nature" is the one that interferes with radio technologies: on November 4th 2015, around 14:30 UT, several Air Traffic Radar stations in western European countries (Sweden, Norway, Belgium and possibly others) suffered from disturbances for a short period of time (several periods spread over about an hour). The degree of disturbances was not equal from countries to countries. A team of astronomers and aeronautical experts from different institutes, including the Royal Observatory of Belgium, has investigated what happened on that day and submitted the results to the Journal of Space Weather and Space Climate.

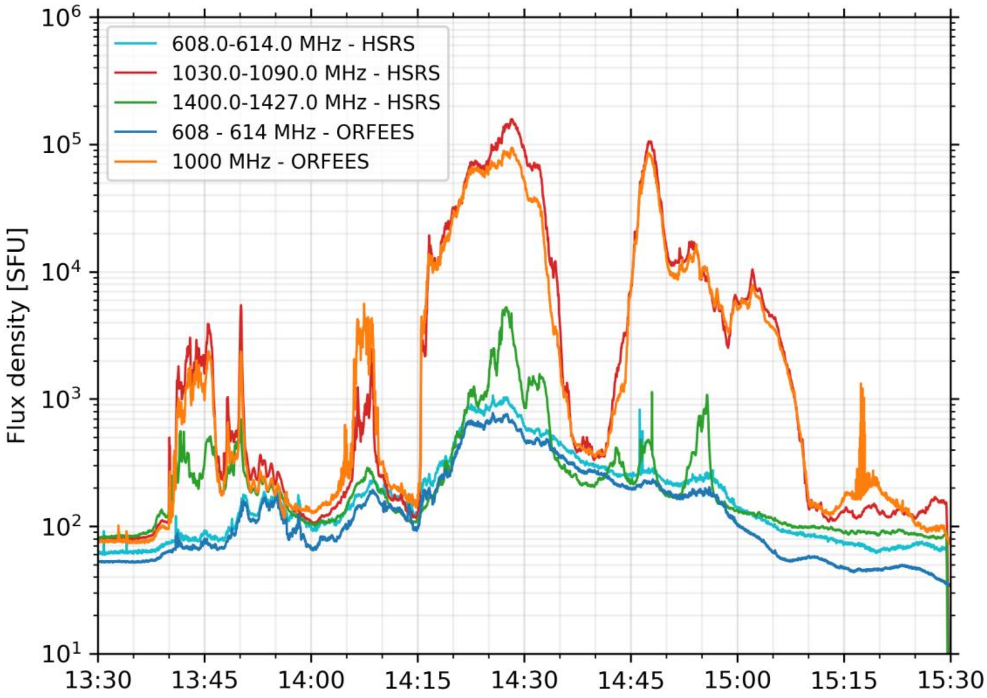

Light curves of the radio burst as seen by the HSRS (Humain, Belgium) and ORFEES (Nançay, France) instruments. The orange and red curves correspond to frequencies very close to the ones where Secondary Surveillance Radars operate. The other light curves near 600 and 1400 MHz show that this radio burst was especially strong in a narrow frequency range between 1000 and 1200 MHz

Shortly before the disturbances started, the Sun produced a flare in an active region close to the central meridian. The flare, which occurred around 13:50UT, was ranked as an M-class event, which is relatively strong but by no mean exceptional. Forty minutes later, radio observatories in Belgium, France and Switzerland registered what is called a type IV burst, which is the signature of energetic electrons trapped in post flare loops (new magnetic arcades forming in the aftermath of a flare). What made this radio event peculiar was its exceptional magnitude in a frequency range between ~1000 and 1200 MHz. By cross calibrating their observations in Humain (Belgium), Nançay (France) and Bleien (Switzerland) scientists could estimate the magnitude of the radio burst to be between 100 000 and 150 000 Solar Flux Units in this narrow frequency range. This represents up to 2000 times the typical intensity of the radio quiet Sun. As shown in the figure above, there were two periods of intense radio emission within half an hour.

Air Traffic Radar stations that were affected are the ones operating Secondary Surveillance radars which send coded queries to the plane avionics to collect information about the aircraft. They operate in two frequency bands 1030 and 1090 MHz which are close to the frequency peak of the radio burst that occurred on that day. Disturbances were seen as ghost echoes lining up with the direction of the Sun.

Explaining why the burst was so intense is not easy. Observations showed that near the peak of the burst, numerous, fine and intense radio structures were observed over a more classical background of emission (see figure below).

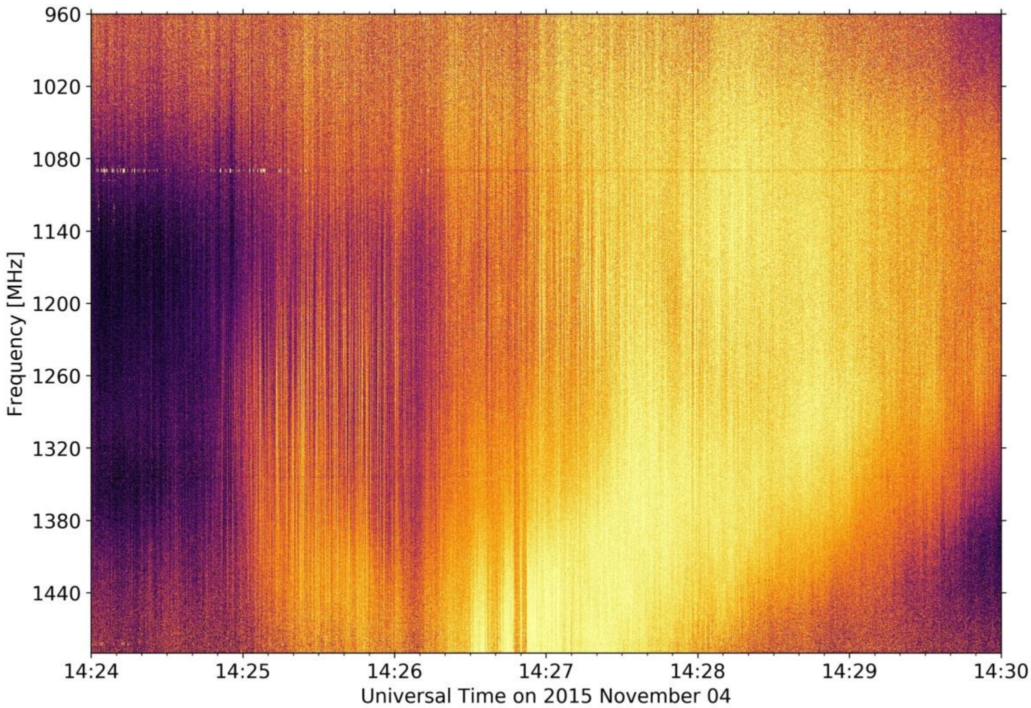

Dynamic spectrum of the radio burst near the peak of the event by the HSRS instrument in Humain. One can see the very fine spectral (vertical) structures of which the burst is made, which are called pulsations. The fine horizontal line near 1080 MHz correspond actually to one of the two bands used in Secondary Surveillance Radar applications

Such intense bursts can occur approximately every two years over the duration of a typical solar cycle, and this one was the strongest since March 2012. However, the frequency band at which the peak will occur remains highly variable and might not fall within the band of radars. In the same study, the team also reported problems with radio devices used during landing by an aircraft in Greenland.

Other services like GNSS (GPS or Galileo) are also known to be sensitive to solar radio burst effects. Beside its radio astronomy facility in Humain, ROB also monitors in near real time the influence of Solar Radio Bursts on GNSS.

Detection of Quasi-Periodic Pulsations in Solar EUV Time-series

Quasi-periodic pulsations (QPPs) are oscillations that have been detected in the integrated solar or stellar emission during flares. QPPs were first detected in the end of the sixties and were, for several decades, only observed in the hard X-rays (HXR) and radio wavelength.

However, a new generation of space instruments allowed extending the detection of QPPs to other parts of the solar spectrum. In particular, the Large Yield Radiometer (LYRA) onboard the PRoject for On-Board Autonomy 2 (PROBA2), an instrument of which the Royal Observatory of Belgium has the PI-ship, reported QPPs in the soft X-rays (SXR) and extreme ultraviolet (EUV) emission of the million-degree solar corona.

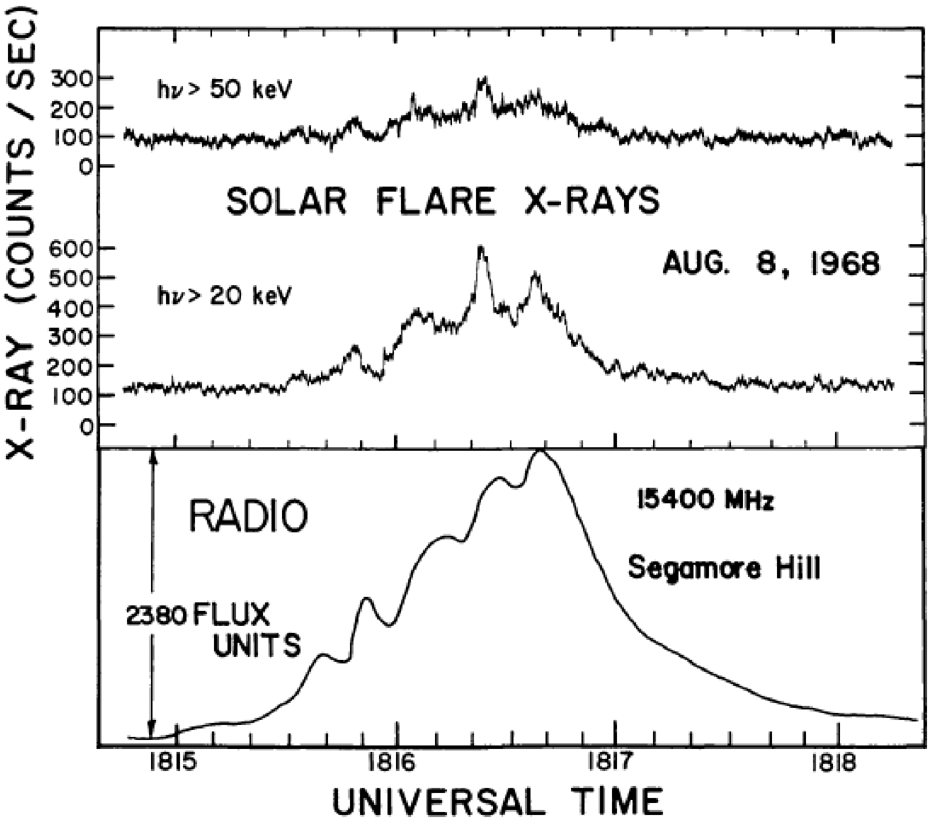

First detection of QPPs by Parks and Winckler in 1969

As this instrument observes the full Sun "as-a-star" instead of focusing on a specific region of interest, and does that on a quasi-uninterrupted way, it recorded most of the flares that happened during the 24th solar cycle and offered the possibility to perform a statistical survey of the QPP phenomenon. Such surveys, which were not possible with the sporadic observations from the old generation of instruments, might help us to better understand the origin of QPPs, and the flaring process itself.

Unfortunately, the amplitude of QPPs in the SXR and EUV spectral ranges is much smaller than in the HXR and radio ranges. Therefore, it is often needed to pre-process the time-series to amplify the oscillation amplitude to allow their detection. Such pre-processing techniques, known as "detrending", have been regularly used in this context, but they come with a risk: they can result in spurious QPP detections and invalidate the conclusions of the statistical survey.

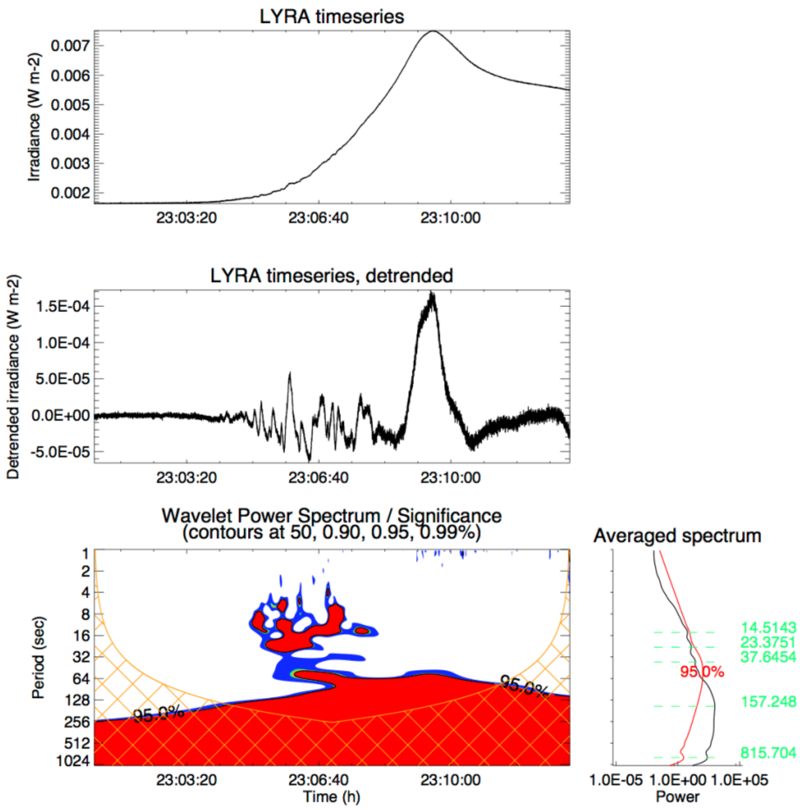

Detection of QPPs with several periods from the LYRA pre-processed times-series.

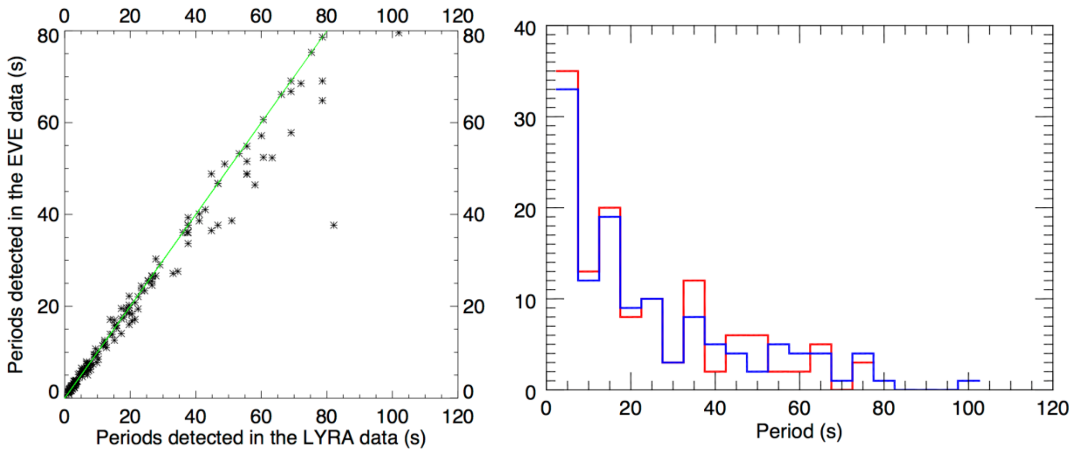

Left panel: correlation of the periods detected in the EVE and LYRA data for 90 flares of the solar cycle 24 of class above M5. Right panel: histogram of all periods detected in these flares that were observed by LYRA (blue) and EVE (red)

A team of scientists, led by M. Dominique from the Royal Observatory of Belgium, proposed a set of criteria to help identifying real QPP detections from pre-processed time-series and discard artefacts. They also applied these criteria to 90 flares stronger that the M5.0 class that had been observed by SDO/EVE/ESP and PROBA2/LYRA to search for QPPs with periods between 1 and 100s. They confirmed that most of the flares exhibit such QPPs, but they found no dependence on the flare longitude or the flare class.

Communication and Information service

The Communication and Information Service aims to communicate and promote the Observatory's research activities and heritage, and also to provide and relay scientific information to the public and the personal.
The activities of the service consist of several tasks: answering questions and inquiries from public, administrations, authorities and press, assisting in all kind of outreach activities such as the Open Doors, exhibition and other events, collaborating with the Planetarium, publishing the Yearbook and the annual report, managing the archives and museum and sending press releases and preparing of texts for printing or for the web site (http://www.astro.oma.be/en/news/).

Information to public, media and authorities

In 2017, the Communication and Information Service answered to about 517 questions from the public sent to by email (253), telephone (more than 206) or by letter or fax (58). 8 questions were also sent via Facebook messages. As usual most questions were about sunset and sunrise, astronomical phenomena, calendar and time-related matters and the history of the Observatory. Since June 2017, the service has its own email account: rob_info@oma.be.

The service gives on numerous occasion information to the media (TV, radio, written press and agencies). Other members of the Observatory appeared in news items on other topics (solar activity, space weather, seismic activity, gravimeter record on Membach, 50th anniversary of the atomic second…).

Since March 2017, guided tours of the Observatory are no more organised for the public. However, there are still some group visits on special occasions. The Communication and Information service also participated to the first edition of the observation stages aimed to 15-18 years teenagers. The individual visitors were mainly journalists, other media related people amateur astronomers with a specific demand and/or students. The service presented the 'History and activities of the ROB' as an introductory talk to some of the visiting groups and guided these in the museum and the dome(s).

Website, news, press releases and social media

Starting January 2017, the results of the new tool for web site analytics and statistics became available for the web pages of the Communication and Information service. However, due to server problems that occurred several times this year, it is not possible to have precise statistics. The data collected indicate 217841 visits on the main website (https://www.astro.oma.be, comprising the information service website). Peaks of visits appear at some periods, noticeable near the dates of the winter solstice and the dates of the daylight saving time.

The content of web pages with the answers to frequently asked questions was regularly updated. For 2017, the pages and data on daylight saving time and position of the sun during the year had at least one update or revision. Since 2017, information about religious calendars are removed from the website. The pages on the celestial phenomena of the month were revised on a regular basis. The service initiated or assisted in sending press releases and putting new items on the website. In 2017 there were 14 topics published (always in 3 languages: NL/FR/EN), including 4 press releases.

From 14 December 2016, the Royal Observatory of Belgium has its own Facebook page (https://www.facebook.com/ORBKSB/) and Twitter account (https://twitter.com/ORB_KSB). In these accounts are published posts and tweets related to the Royal Observatory of Belgium. On 31 December 2017, the ROB Facebook webpage has 290 likes and 316 followers, while the Twitter accounts got 217 followers. The numbers of likes and followers increases steadily. From 14 November 2017, the Observatory has also its YouTube account. On 31 December 2017, there are 5 videos, a number which is expected to increase in the future.

Night of the Shooting Stars (cancelled)

A third edition of the night of the shooting stars was organized for Wednesday evening 9 August 2017. The Planetarium was the main organizer of this event, with the Royal Observatory of Belgium and the Royal Belgian Institute for Space Aeronomy assisting. The Communication and Information service participated to the organization by sharing and updating news of the event and by organizing conferences and by managing the logistics. However, because of bad weather the event was cancelled on Tuesday August 8. The announcement of the cancellation was sent to all the participants.

Exhibitions

As each year, the Royal Palace in Brussels opened its doors to the public in summer: in 2017 from 22 July to 3 September. The public could discover the exposition "HEAVEN!" allowing visitors to rediscover the sky in all its aspects: works of art inspired by the sky, unusual objects, scientific observation or measurement instruments, video sequences, etc. The Royal Observatory of Belgium provided three objects of its museum collection, three armillary spheres designed by Jérôme de Lalande in the 18th century, and a surprising picture of the Milky Way composed with the Gaia satellite data. A special homage to our colleague Dr. Jan Cuypers is given during the exhibition. Jan Cuypers, astronomer and astrophysicist, suddenly passed on February 28, 2017. As chief of the Communication and Information Service, he had proposed the theme of the heaven/sky for this year. He also had contributed to the choice of the pieces of the Observatory for the exhibition, in collaboration with Hilde Langenaken. An In Memoriam is placed next to the map of the Milky Way and contains a short biography of Jan Cuypers.

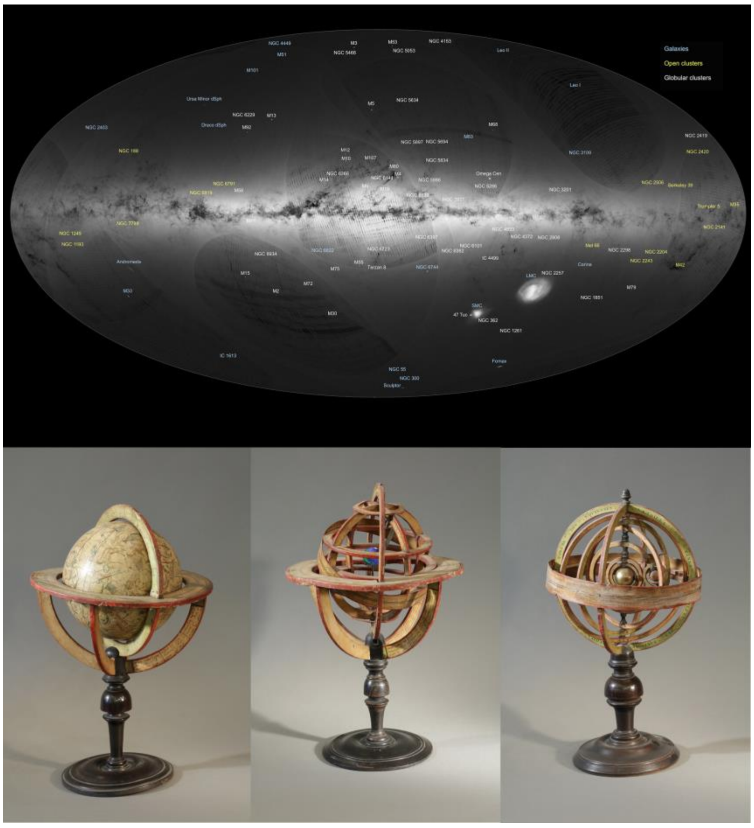

Above: One billion star map of our galaxy created with the optical telescope of the satellite Gaia (Credit: ESA/Gaia/DPAC). Below: Three armillary spheres designed by Jérôme de Lalande in 1775. Left: the spherical sphere; in the centre: the geocentric model of our solar system (with the Earth in the centre); right: the heliocentric model of our solar system (with the Sun in the centre)

The Planetarium

Highlights in 2017

In 2017, the Planetarium welcomed 41,207 visitors to one of its daily sessions or school classes, a slight increase of +3.9% (+1537 visitors) compared to the previous year.

The Planetarium website was visited 116,260 times (82,074 different visitors, +29.6% compared to 2016), for a total of 1,549,715 hits.

Special activities

- Electronic music concert on February 18 with Meteor Music
- Prestigious partnership with the Brussels Philharmonic Orchestra leading to 2 concerts on March 2 and 3
- Selection of the laureates of the BIFROST-ONE competition (creation by secondary school students of a scientific experiment to be conducted during a 0-g flight) in partnership with the Brussels Region on 22 March
- Conference (Prof. Pasquale Nardone) for ESERO teachers on April 18
- Hosting of the groups participating to the ASGARD project on April 20
- Partnership with the Kunstenfestivaldesarts, leading to 3 performances of an original theatrical creation (May 6, 7 and 8)
- Special sessions for Asteroid Day on June 30
- Participation in the Zonnekijkdag on July 2nd
- Night of the Stars on August 9 at the Observatory (cancelled)
- Poetry under the Stars on September 8
- FNRS / ROB Astronomy Contact Group Day on September 19
- Participation in the Nocturnes des Musées bruxellois on September 28
- Night of the Darkness (Nuit de l'Obscurité/Nacht van de Duisternis) on October 14
- Dirk Frimout Jubilee on October 25
- Teachers' Day on October 27
- Electronic music concert on November 24
- Participation in the Dag van de Wetenschap on November 26
- Launch of the new full-dome film EXPLORE on December 20
- Room rentals for BeSpace (March 10), VITO (March 14), VVS (April 22), FFAAB (April 22), Sony (May 30), IRM (October 4), SIDC (October 6), UPV (October 11), Mechelen Cultural Centre (December 23).

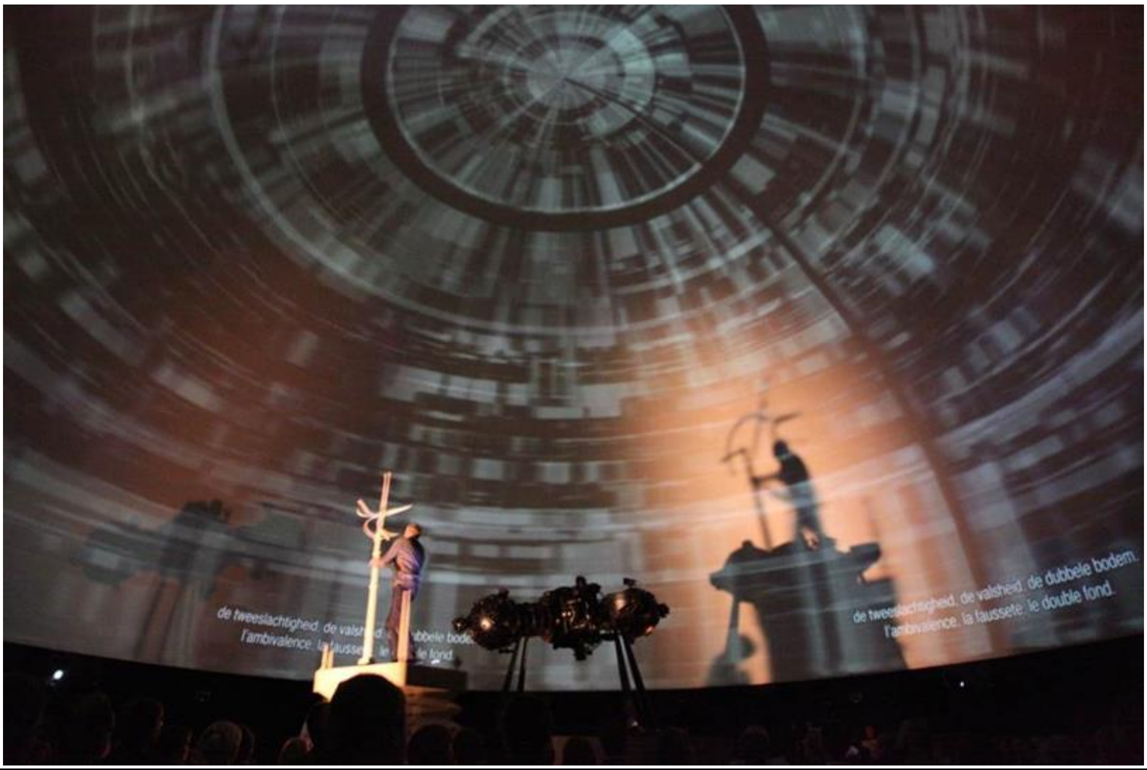
de tweeslachtigheid, de valsheid, de dubbele bodem.
l'ambivalence, la fausseté, le double fond.

Annex 1: Publications

Publications with peer review

[1] Andrade L., Janot-Pacheco E., Emilio M., Frémat Y., Neiner C., Poretti E., Mathias P., Rainer M., Suárez J. C., Uytterhoeven K., Briquet M., Diago P. D., Fabregat J., Gutiérrez-Soto J.
Photometric and spectroscopic variability of the B5IIIe star HD 171219
A&A, 603, A41 (2017). DOI: 10.1051/0004-6361/201629177

[2] Baland, R.-M., Yseboodt, M., Rivoldini, A., Van Hoolst, T.
Obliquity of Mercury: Influence of the precession of the pericenter and of tides
Icarus. 291, pp. 136-159 (2017). DOI: 10.1016/j.icarus.2017.03.020

[3] Bennitt, G. V., Johnson, H.R., Weston, P. P., Jones, J., Pottiaux, E.
An assessment of ground-based GNSS Zenith Total Delay observation errors and their correlations using the Met Office UKV model
Quarterly Journal of Meteorological Society, 143 issue 707, pp. 2436–2447 (2017). DOI: 10.1002/qj.3097.

[4] Blomme, R., Fenech, D. M., Prinja, R. K., Pittard, J. M., Morford, J. C.
Variable millimetre radiation from the colliding-wind binary Cygnus OB2 #8A
Astronomy and Astrophysics, 608, A69 (2017). DOI: 10.1051/0004-6361/201731403

[5] Bozdağ E., Ruan Y., Metthez N., Khan A., Leng K., van Driel M., Wieczorek M., Rivoldini A., Larmat C. S., Giardini D., Tromp J., Lognonné P., Banerdt B. W.
Simulations of Seismic Wave Propagation on Mars
Space Science Reviews (2017). DOI: 10.1007/11214-017-0350-z

[6] Bozzo, E., Oskinova, L., Lobel, A., Hamann, W.-R.
The super-orbital modulation of supergiant high-mass X-ray binaries
A&A, 606, L10 (2017).

[7] Bruyninx C., Altamimi Z., Brockmann E., Caporali A., Dach R., Dousa J., Fernandes R., Giannou M., Habrich H., Ihde J., Jivall L., Kenyeres A., Lidberg M., Pacione R., Poutanen M., Szafranek K., Söhne W., Stangl G., Torres J., Völksen C.
Implementation of the ETRS89 in Europe: Current Status and Challenges
In: International Association of Geodesy Symposia, “REFAG2014, Proceedings of the IAG Commission 1 Symposium Kirchberg, Luxembourg, 13–17 October, 2014”, pp. 135-145, doi: 10.1007/1345_2015_130

[8] Caudron, C., Campion, R., Rouwet, D., Lecocq, T., Capaccioni, B., Syahbana, D., Suparjan, S., Purwanto, B., Bernard, A.
Stratification at the Earth's largest hyperacidic lake and its consequences
Earth and Planetary Science Letters, 459 (2017). DOI: 10.1016/j.epsl.2016.11.002

[9] Chatzinikos M., Dermanis A.
Interpretation of numerically detected rank defects in GNSS data analysis problems in terms of deficiencies in reference system definition
GPS Solutions, Vol. 21, Issue 3, pp. 1239-1250 (2017).

[10] Chatzinikos M., Kotsakis C.
Noise Filtering Augmentation of the Helmert Transformation for the Mapping of GNSS-Derived Position Time Series to a Target Frame
In: Freymueller J.T., Sánchez L. (eds) International Symposium on Earth and Environmental Sciences for Future Generations. International Association of Geodesy Symposia, vol. 147, pp. 277-283 (2017).

[11] Chatzinikos M., Kotsakis C.
Appraisal of the Hellenic Geodetic Reference System 1987 based on backward-transformed ITRF coordinates using a national velocity model
Survey Review, Vol. 49, pp. 386-398 (2017).

[12] De Cat P.
7 positions of minor planets observed before 2017
Minor Planet Circulars Supplement 826400 (2017).

[13] Defraigne P., Huang W., Bertrand B., Rovera D.
Study of the GPS inter-frequency calibration of timing receivers
Metrologia, vol 55, num 1 (2017).

[14] Dehant V., Laguerre R., Rekier J., Rivoldini A., Triana S.A., Trinh A., Van Hoolst T., Zhu P.
Understanding the effects of the core on the nutation of the Earth
Geodesy and Geodynamics, 8(6), pp. 389-395 (2017). DOI: 10.1016/j.geog.2017.04.005

[15] Dehant V., Park R., Dirkx D., Iess L., Neumann G., Turyshev S., Van Hoolst T.
Survey of capabilities and applications of accurate clocks: directions for planetary science
Space Science Reviews, 212(3), pp. 1433-1451 (2017). DOI: 10.1007/s11214-017-0424-y

[16] D'Huys E., Seaton D.B., De Groof A., Berghmans D., Poedts S.
Solar signatures and eruption mechanism of the 2010 August 14 CME
Journal of Space Weather and Space Climate, Vol 7 (2017).

[17] Dorn C., Venturini J., Khan A., Heng K., Alibert Y., Helled R., Rivoldini A., Benz W.
A generalized Bayesian inference method for constraining the interiors of super Earths and sub-Neptunes
Astronomy and Astrophysics, 597 (2017). DOI: 10.1051/0004-6361/201628708

[18] Drews R., Pattyn F., Hewitt I. J., Matsuoka K., Helm V., Berger S., Bergeot N. and Favier L.
Hydrological coupling between subglacial water conduit, esker, and ice-shelf channel across the grounding line of an Antarctic ice shelf
Nature Communications, 8 (2017). DOI: 10.1038/ncomms15228

[19] Dumbovic, M., Srivastava, N., Khodia, Y., Vrsnak, B., Devos, A., Rodriguez, L.
Validation of the CME Geomagnetic forecast alerts under the COMESEP alert system
Solar Physics, 292 issue 8, pp. 96 (2017). DOI: 10.1007/s11207-017-1120-5

[20] Dumoulin C., Tobie G., Verhoeven O., Rosenblatt P., Rambaux N.
Tidal constraints on the interior of Venus
Journal of Geophyscial Research: Planets, Volume 122, issue 6, pp. 1338-1352 (2017).

[21] Fenech, D. M., Clark, J. S., Prinja, R. K., Morford, J. C., Dougherty, S., Blomme, R.
ALMA observations of the supergiant B[e] star Wd1-9
MNRAS 464, L75

[22] Ferland, G. J.,Chatzikos, M., Guzmán, F., Lykins, M. L., van Hoof, P. A. M., Williams, R. J. R., Abel, N. P., Badnell, N. R., Keenan, F. P., Porter, R. L., Stancil, P. C.
The 2017 Release Cloudy
Revista Mexicana de Astronomía y Astrofísica Vol. 53, pp. 385-438 (2017).

[23] Frémat, Y., Altmann, M., Pancino, E., Soubiran, C., Jofré, P., Damerdji, Y., Heiter, U., Royer, F., Seabroke, G., Sordo, R., Blanco-Cuaresma, S., Jasniewicz, G., Martayan, C., Thévenin F., Vallenari, A., Blomme, R., David, M., Gosset, E., Katz, D., Viala, Y., Boudreault, S., Cantat-Gaudin, T., Lobel, A., Meisenheimer, K., Nordlandet, T., Raskin, R., Royer, P., Zorec, J.,
A test field for Gaia. Radial velocity catalogue of stars in the South Ecliptic Pole
A&A, 597, 10 (2017).

[24] Gaia Collaboration, Clementini, G., Eyer, L., Ripepi, V., Marconi, M., Muraveva, T., Garofalo, A., Sarro, L. M., Palmer, M., Luri, X., and 576 coauthors, including Blomme, R., Cuypers, J., Frémat, Y., Pauwels, T., De Cat, P., Lobel, A.
Gaia Data Release 1. Testing parallaxes with local Cepheids and RR Lyrae stars
Astronomy & Astrophysics, 605 issue A79, pp. 1-29 (2017). DOI: 10.1051/0004-6361/201629925

[25] Gaia Collaboration, van Leeuwen, F., Vallenari, A., Jordi, C., Lindegren, L., Bastian, U., Prusti, T., de Bruijne, J. H. J., Brown, A. G. A., Babusiaux, C., and 582 coauthors, including Blomme, R., Cuypers, J., Frémat, Y., Pauwels, T., De Cat, P., Lobel, A.
Gaia Data Release 1. Open cluster astrometry: performance, limitations, and future prospects
Astronomy & Astrophysics, 601 issue A19, pp. 1-65 (2017). DOI: 10.1051/0004-6361/201730552

[26] Gillmann C., Golabek G., Tackley P., Raymond S.
The role of Late Veneer impacts in the evolution of Venus
EPSC abstract, Vol. 11, EPSC2017-15 (2017).

[27] Goldman S.R., van Loon J.Th., Zijlstra A.A., Green J.A., Wood P.R., Nanni A., Imai H., Whitelock P.A., Matsuura M., Groenewegen M.A.T., Gomez J.F.
The wind speeds, dust content, and mass-loss rates of evolved AGB and RSG stars at varying me-tallicity
MNRAS 465, 403 (2017).

[28] Groenewegen M.A.T.
The photodissociation of CO in circumstellar envelopes
A&A 606, A67 (2017).

[29] Groenewegen, M.A.T., Jurkovic, M.
Luminosities and infrared excess in Type II and anomalous Cepheids in the Large and Small Magellanic Clouds
A&A 603, A70 (2017).

[30] Groenewegen M.A.T., Jurkovic, M.
The period - luminosity and period -radius relations of Type II and anomalous Cepheids in the Large and Small Magellanic Clouds
A&A 604, A29 (2017).

[31] Gupta, S., Collier, J., Garcia-Moreno, D., Oggioni, F., Trenteseaux, A., Vanneste, K., De Batist, M., Camelbeeck, T., Potter, G., Van Vliet-Lanoë, B., Arthur, J.
Two-stage opening of the Dover Strait and the origin of island Britain
Nature Communications, 8 (2017). DOI: 10.1038/ncomms15101

[32] Guzmán F., Badnell N.R., Williams R.J.R., van Hoof P.A.M., Chatzikos M., Ferland G.J.
H, He-like recombination spectra II: l-changing collisions for He Rydberg states
MNRAS, 464, 312 (2017).

[33] Guzmán F., Badnell N.R., Chatzikos M., van Hoof P.A.M., Williams R.J.R., Ferland G.J.
Testing atomic collision theory with the two-photon continuum of astrophysical nebulae
MNRAS, 467, 3944 (2017).

[34] Hamlaoui M., Vanneste K., Baddari K., Louail L., Vleminckx B., Demdoum A.
Probabilistic seismic hazard assessment in the northeastern part of Algeria
Arabian Journal of Geosciences, June 2017, 10:238 (2017).

[35] Herique, A., Agnus, B., Asphaug, E., Barucci, A., Beck, P., Bellerose, J., Biele, J., Bonal, L., Bousquet, P., Bruzzone, L., Buck, C., Carnelli, I., Cheng, A., Ciarletti, V., Delbo, M., Du, J., Du, X., Eyraud, C., Fa, W., Gil Fernandez, J., Gassot, O., Granados-Alfaro, R., Green, S.F., Grieger, B., Grundmann, J.T., Grygorczuk, J., Hahnel, R., Heggy, E., Ho, T-M., Karatekin, Ö., Kasaba, Y., Kobayashi, T., Kofman, W., Krause, C., Kumamoto, A., Küppers, M., Laabs, M., Lange, C., Lasue, J., Levasseur-Regourd, A.C., Mallet, A., Michel, P., Mottola, S., Murdoch, N., Mütze, M., Oberst, J., Orosei, R., Plettemeier, D., Rochat, S., RodriguezSuquet, R., Rogez, Y., Schaffer, P., Snodgrass, C., Souyris, J-C., Tokarz, M., Ulamec, S., Wahlund, J-E., Zine, S.,
Direct Observations of Asteroid Interior and Regolith Structure: Science Measurement Requirements
Advances in Space Research (2017). DOI: https://doi.org/10.1016/j.asr.2017.10.020

[36] Hrivnak B. J., Van Winckel, H. Van de Steene G.C., Bohlender D., Sperauskas J., Wenxian L.
Where are the Binaries? Results of a Long-term Search for Radial Velocity Binaries in Proto-planetary Nebulae
ApJ, 846, 96 (2017).

[37] Hrudková M., Hatzes A., Karjalainen R., Lehmann H., Hekker S., Hartmann M., Tkachenko A., Prins S., Van Winckel H., De Nutte R., Dumortier L., Frémat Y., Hensberge H., Jorissen A., Lampens P., Laverick M., Lombaert R., Pápics P. I., Raskin G., Sódor Á., Thoul A., Van Eck S., Waelkens C.
The discovery of a planetary candidate around the evolved low-mass Kepler giant star HD 175370
MNRAS, 464, pp. 1018 (2017). DOI: 10.1093/mnras/stw2379

[38] Hyodo R., Rosenblatt P., Genda H., Charnoz S.
On the impact origin of Phobos and Deimos II: True polar wander and disk evolution
The Astrophysical Journal, Vol. 851, N° 2 (2017).

[39] Hyodo R., Genda H., Charnoz S., Rosenblatt P.
On the impact origin of Phobos and Deimos I: Thermodynamic and physical properties of the proto-Martian moons disk
The Astrophysical Journal, doi.org/10.3847/1538-4357/aa81c4, 845:125, 8 pp. (2017).

[40] Kačmařík M., Douša J., Dick G., Zus F., Brenot H., Möller G., Pottiaux E., Kapłon J., Hordyniec P., Václavovic P., Morel L.
Inter-technique validation of tropospheric slant total delays
Atmospheric Measurement Techechnique (AMT), 10, pp. 2183-2208 (2017). DOI: 10.5194/amt-10-2183-2017

[41] Kahraman Aliçavuş, F., Niemczura, E., Polińska, M., Hełminiak, K. G., Lampens, P. et al.
High-resolution spectroscopy and abundance analysis of delta Scuti stars near the gamma Doradus instability strip
MNRAS, 470, pp. 4408 (2017). DOI: DOI: 10.1093/mnras/stx1498

[42] Katsiyannis, A., Dominique, M., Pierrard, V., Lopez Rosson, G., De Keyser, J., Berghmans, D., Kruglanski, M., Dammasch, I., De Donder, E.
The detection of ultra-relativistic electrons in low Earth orbit
Journal of Space Weather and Space Climate, 8 (2017).

[43] Kerschbaum F., Maercker M., Brunner M., Lindqvist M., Olofsson H., Mecina M., De Beck E., Groenewegen M.A.T., Lagadec E., Mohamed S., Paladini C., Ramstedt S., Vlemmings W.H.T., Wittkowski M.
Rings and filaments: The remarkable detached CO shell of U Antliae
A&A 605, A116 (2017). DOI : 10.1051/0004-6361/201730665

[44] Knuts, E., Hinzen, K.-G., Reamer, S.K., Camelbeeck, T.
A Nineteenth-Century National Prussian Macroseismic Questionnaire
Seismological Research Letters, 89 (1): 191–201 (2017). DOI: 10.1785/0220170199

[45] Kotsakis C., Chatzinikos M.,
Rank defect analysis and the realization of proper singularity in normal equations of geodetic networks
Journal of Geodesy, Vol. 91, Issue 6, pp. 627-652 (2017).

[46] Lainey V., Jacobson R.A., Tajeddine R., Cooper N.J., Murray C., Robert V., Tobie G., Guillot T., Mathis S., Remus F., Desmars J., Arlot J.-E., De Cuyper J.-P., Dehant V., Pascu D., Thuillot W., Le Poncin-Lafitte Ch., Zahn J.-P.
New constraints on on Saturn's interior from Cassini astrometric data
Icarus, 281, pp. 286-296 (2017). DOI: 10.1016/j.icarus.2016.07.014

[47] Lampens, P., Frémat, Y., Vermeylen, L., Sòdor, À., Skarka, M., De Cat, P., Bognàr, Zs., De Nutte, R., Dumortier, L., Escorza, A., Oomen, G. M., Van de Steene, G., Kamath, D., Laverick, M., Samadi, A., Triana, S., Lehmann, H.
Multi-technique investigation of the binary fraction among A-F type candidate hybrid variable stars discovered by Kepler
A&A, 610, A17 (2017). DOI: 10.1051/0004-6361/201730694 [arXiv:1709.03436]

[48] Lampens, P., Van Cauteren, P., Ayiomamitis, A., Kleidis, S., Panagiatopoulos, K. Vanleenhove, M., Hambsch, J., Hautecler, H., Van Wassenhove, J., Vermeylen, L.
Times of Minima of 116 eclipsing binary systems (2010-2015)
IBVS N° 6230, 1 (2017).

[49] Lecocq, T., Camelbeeck, T.
Electrical Resistivity Tomography data across the Hockai Fault Zone (Ardenne, Belgium)
Data in Brief (2017).

[50] Lecocq, T., Longuevergne, L., Pedersen, H., Brenguier, F., Stammler, K.
Monitoring ground water storage at mesoscale using seismic noise: 30 years of continuous observation and thermo-elastic and hydrological modeling
Scientific Reports, 7 issue 1, pp. 14241 (2017). DOI: 10.1038/s41598-017-14468-9

[51] Lemasle B., Groenewegen M.A.T., Grebel E.K., Bono G., Fiorentino G., Francois P., Inno L., Kovtyukh V.V., Matsunaga N., Pedicelli S., Primas F., Pritchard J., Romaniello M., da Silva R.
Detailed chemical composition of classical Cepheids in the LMC cluster NGC 1866 and in the field of the SMC
A&A 608, A85 (2017).

[52] Lobel A., Royer P., Martayan C., Laverick M., Merle T., David M., Hensberge H., Thienpont E.
The Belgian repository of fundamental atomic data and stellar spectra
Canadian Journal of Physics, Volume 95, Number 9 (2017). DOI : 10.1139/cjp-2016-0750

[53] Marconi M., Molinaro R., Ripepi V., Cioni M.-R.L., Clementini G., Moretti M.I., Ragosta F., de-Grijs R., Groenewegen M.A.T., Ivanov V.D.
The VMC Survey XXIII. Model fitting of light and radial velocity curves of Small Magellanic Cloud classical Cepheids
MNRAS 466, 3206 (2017).

[54] Marigo P., Girardi L., Bressan A., Rosenfield P., Aringer B., Chen Y., Dussin M., Nanni A., Pastorelli G., Rodrigues T.S., Trabucchi M., Bladh S., Dalcanton J., Groenewegen M.A.T., Montalban J., Wood P.R.
A New Generation of PARSEC-COLIBRI Stellar Isochrones Including the TP-AGB Phase
ApJ 835, 77 (2017).

[55] Mayer P., Harmanec P., Chini R., Nasseri A., Nemravová J. A., Drechsel H., Catalan-Hurtado R., Barlow B. N., Frémat Y., Kotková L.
Physical properties of seven binary and higher-order multiple OB systems
Astronomy and Astrophysics, 600, A33 (2017).

[56] McQuinn K.B.W., Boyer M.L., Mitchell M.B., Skillman E.D., Gehrz R.D., Groenewegen M.A.T., McDonald I., Sloan G.C., van Loon J.Th., Whitelock P.A., Zijlstra. A.A.
DUSTiNGS III: Distribution of Intermediate-Age and Old Stellar Populations in Disks and Outer Extremities of Dwarf Galaxies
ApJ 834, 78 (2017).

[57] Merle, T., Van Eck, S., Jorissen, A., Van der Swaelmen, M., Masseron, T., Zwitter, T., Hatzidimitriou, D., Klutsch, A., Pourbaix, D., Blomme, R., and 28 coauthors
The Gaia-ESO Survey: double-, triple-, and quadruple-line spectroscopic binary candidates
A&A 608, A95 (2017).

[58] Michal, K., Douša, J., Dick, G., Zus, F., Brenot, H., Möller, G., Pottiaux, E., Kapłon, J., Hordyniec, P., Václavovic, P., Morel, L.
Inter-technique validation of tropospheric slant total delays
Atmos. Meas. Tech., 10, pp. 2183-2208 (2017). DOI: 10.5194/amt-10-2183-2017

[59] Michel, P., Kueppers, M., Sierks, H., Carnelli, I., Cheng, A. F., Mellab, K, Granvik, M., Kestila, A., Kohout, T., Muinonen, K., Nasilak, A., Penttila, A., Tikka, T., Tortora, P., Ciarletti, V., Herique, A., Murdoch, N., Asphaug, E., Rivkin, A., Barnouin, O., Bagatin, A. C., Pravec, P., Richardson, D. C., Schwartz, S. T., Tsiganis, K., Ulamec, S., Karatekin, Ö.
European component of the AIDA mission to a binary asteroid: Characterization and interpretation of the impactof the DART mission
Adv. Space Res. (2017). DOI: 10.1016/j.asr.2017.12.020

[60] Moestl, C., Isavnin, A., Boakes, P., Kilpua, E. K. J., Davies, J., Harrison, R., Barnes, D., Krupar, V., Eastwood, J., Good, S., Forsyth, R., Bothmer, V., Reiss, M., Amerstorfer, T., Winslow, R., Anderson, B., Philpott, L., Rodriguez, L., Rouillard, A., Gallagher, P., Nieves-Chinchilla, T., Zhang, T.
Modeling observations of solar coronal mass ejections with heliospheric imagers verified with the Heliophysics System Observatory
Space Weather, 15 issue 7, pp. 955-970 (2017). DOI: 10.1002/2017SW001614

[61] Morosan, D, Gallagher, P, Fallows, R, Reid, H, Mann, G, Bisi, M, Magdalenic, J, Rucker, H, Thidé, B, Vocks, C, and 49 coauthors
The association of a J-burst with a solar jet
Astronomy & Astrophysics, 606 (2017). DOI: 10.1051/0004-6361/201629996

[62] Müller, D., Nicula, B., Felix, S., Verstringe, F., Bourgoignie, B., Csillaghy, A., Berghmans, D., Jiggens, P., García-Ortiz, J. P., Ireland, J., Zahniy, S., Fleck, B.
JHelioviewer. Time-dependent 3D visualisation of solar and heliospheric data
Astronomy & Astrophysics, 606 issue October 2017, pp. 13 (2017). DOI: 10.1051/0004-6361/201730893

[63] Murdoch, N., Hempel, S. Pou, L., Cadu, A., Garcia, R. F., Mimoun, D., Margerin, L., Karatekin, Ö.
Probing the internal structure of the asteriod Didymoon with a passive seismic investigation
Planetary and Space Science, Volume 144, p. 89-105. (2017).

[64] Namaoui, H., Kahlouche, S, Belbachir, A. H., Van Malderen, R., Brenot, H., Pottiaux, E.
GPS water vapour and its comparison with radiosondes and ERA- Interim reanalysis in Algeria
Advances in Amospheric Sciences, 34 issue 5, pp. 623–634 (2017). DOI: 10.1007/s00376-016-6111-1

[65] Noack L., Rivoldini A., Van Hoolst T.
Volcanism and outgassing of stagnant-lid planets: Implications for the habitable zone
Physics of the Earth and Planetary Interiors, 269 (2017). DOI: 10.1016/j.pepi.2017.05.010

[66] Otsuka M., Ueta T., van Hoof P.A.M., Sahai R., Aleman I., Zijlstra A.A., Chu Y.-H., Villaver E., Leal-Ferreira M.L., Kastner J., Szczerba R., Exter K.M.
The Herschel Planetary Nebula Survey (HerPlaNS) -- A Comprehensive Dusty Photoionization Model of NGC 6781
ApJS, 231, 22 (2017).

[67] Paladini C., Klotz D., Sacuto S., Lagadec E., Wittkowski M., Richichi A., Hron J., Jorissen A., Groenewegen M.A.T., Kerschbaum F., Verhoelst T., Rau G., Olofsson H., Zhao-Geisler R., Matter A.
The VLTI/MIDI view on the inner mass loss of evolved stars from the Herschel MESS sample
A&A 600, A136 (2017).

[68] Pálinkáš, V., Francis, O., Val'ko, M., Kostelecký, J., Van Camp, M., Castelein, S., Bilker-Koivula, M., Näränen, J., Lothhammer, A., Falk, R., Schilling, M., Timmen, L., Iacovone, D., Baccaro, F., Germak, A., Biolcati, E., Origlia, C., Greco, F., Pistorio, A., De Plaen, R., Klein, G., Seil, M., Radinovic, R., Reudink, R., Dykowski, P., Sękowski, M., Próchniewicz, D., Szpunar, R., Mojzeš, M., Jańk, J., Papčo, J., Engfeldt, A., Olsson, P., Smith, V., van Westrum, D., Ellis, B., Lucero, B.
Regional comparison of absolute gravimeters, EURAMET.M.G-K2 key comparison
Metrologia, 54 (2017). DOI: 10.1088/0026-1394/54/1A/07012

[69] Pancino, E., Lardo, C., Altavilla, G., Marinoni, S., Ragaini, S., Cocozza, G., Bellazzini, M., Sabbi, E., Zoccali, M., Donati, P., and 53 coauthors, including Blomme, R., Lobel, A.
The Gaia-ESO Survey: Calibration strategy
A&A 598, A5 (2017).

[70] Panning M.P., Lognonné P., Banerdt W.B., Garcia R., Golombek M., Kedar S., Knapmeyer-Endrun B., Mocquet A., Teanby N.A., Tromp J., Weber R., Beucler E., Blanchette-Guertin J.-F., Bozdağ E., Drilleau M., Gudkova T. , Khan A., Lekić V., Murdoch N., Plesa A.-C., Rivoldini A., Schmerr N., Ruan Y., Verhoeven O., Gao C., Christensen U., Clinton J., Dehant V., Giardini D., Mimoun D., Pike W.T., Smrekar S., Wieczorek M., Knapmeyer M., Wookey J.
Planned Products of the Mars Structure Service for the InSight Mission to Mars
Space Sci. Rev., 211(1-4), pp. 611-650 (2017). DOI: 10.1007/s11214-016-0317-5

[71] Patel M. et al, included BenMoussa A., Giordanengo B., Gissot S.
NOMAD spectrometer on the ExoMars trace gas orbiter mission: part 2—design, manufacturing, and testing of the ultraviolet and visible channel
Applied Optics, 56 issue 10, pp. 2771-2782 (2017). DOI: 10.1364/AO.56.002771

[72] Perton, M., Spica, Z., Caudron, C.,
Inversion of the horizontal to vertical spectral ratio in presence of strong lateral heterogeneity
Geophysical Journal International (2017).

[73] Podladchikova, T., Van der Linden, R., Veronig, A.
Sunspot number second differences as precursor of the following 11-year sunspot cycle
Astrophysical Journal, 850 issue 1 (2017).

[74] Ripepi V., Cioni M.-R.L., Moretti M.I., Marconi M., Bekki K., Clementini G., de Grijs R., Emer-son J.-P., Groenewegen M.A.T., Ivanov V.D., Molinaro R., Muraveva T., Oliveira J.M., Piatti A.E., Subramanian S., van Loon, J.Th.
The VMC Survey. XXV. The 3D structure of the Small Magellanic Cloud from Classical Cepheids
MNRAS 472, 808 (2017).

[75] Shestov, S. V., Nakariakov, V. M., Ulyanov, A. S., Reva, A. A., Kuzin, S. V.
Nonlinear Evolution of Short-wavelength Torsional Alfvén Waves
The Astrophysical Journal, 840 issue 2, pp. 64 (2017). DOI: 10.3847/1538-4357/aa6c65

[76] Smalley B., Kurtz D.W., Antoci V., Murphy S.J., Holdsworth D.L., De Cat P., Anderson D.R., Catanzaro G., Collier Cameron A., Hellier C., Maxted P.F.L., Norton A.J., Pollacco D., Ripepi V., West R.G., Wheatley P.J.
Pulsation versus metallicism in Am stars as revealed by LAMOST and WASP
Monthly Notices of the Royal Astronomical Society, 465 issue 3, pp. 2662-2670 (2017). DOI: 10.1093/mnras/stw2903

[77] Stankov S.M., Bergeot N., Berghmans D., Bolsée D., Bruyninx C., Chevalier J.-M., Clette F., De Backer H., De Keyser J., D'Huys E., Dominique M., Lemaire J., Magdalenić J., Marqué C., Pereira N., Pierrard V., Sapundjiev D., Seaton D.B., Stegen K., Van der Linden R., Verhulst T.G.W., West M.J.
Multi-instrument observations of the solar eclipse on 20 March 2015 and its effects on the plasmasphere and ionosphere over Belgium and Europe

Journal of Space Weather and Space Climate, 7 issue A19 (2017). DOI: 10.1051/swsc/2017017

[78] Temmer, M., Dissauer, K., Thalmann, J.K., Veronig, A.M., Tschernitz, J., Hinterreiter, J., Rodriguez, L.
Flare-CME characteristics -- effectively relating remote-sensing image data to in-situ measurements supported by modeling
Solar Physics, 292 issue 7, pp. 93.

[79] Thiemann, E., Dominique, M., Pilinski, M., Eparvier, F.
Vertical Thermospheric Density Profiles from EUV Solar Occultations made by PROBA2 LYRA for Solar Cycle 24
Space Weather (2017). DOI: 10.1002/2017SW001719

[80] Triantafyllou, A., Watlet, A., Bastin, C.
Geolokit: An interactive tool for visualising and exploring geoscientific data in Google Earth
International Journal of Applied Earth Observation and Geoinformation, 62, pp. 39-46 (2017). DOI: 10.1016/j.jag.2017.05.011

[81] Triantafyllou, A., Berger, J., Baele, J.-M., Bruguier, O., Diot, H., Ennih, N., Monnier, C., Plissart, G., Vandycke, S., Watlet, A.,
Intra-oceanic arc growth driven by magmatic and tectonic processes recorded in the Neoproterozoic Bougmane arc complex (Anti-Atlas Morocco)
Precambrian Research, 304, pp. 39-63 (2017). DOI: 10.1016/j.precamres.2017.10.022

[82] Turbet M., Forget F., Svetsov V., Tran H., Karatekin O., Popova O., Gillmann C.
The impact of meteoritic impacts on the early Martian environment
EPSC abstract, Vol. 11, EPSC2017-561 (2017).

[83] Turbet M., Forget F., Svetsov V., Tran H., Hartmann J-M, Karatekin O., Gillmann C., Popova O., Head J.
The Environmental Effects of Meteoritic Impacts on Early Mars With a Versatile 3-D Global Climate Model
Fourth International Conference on Early Mars: Geologic, Hydrologic, and Climatic Evolution and the Implications for Life, Proceedings of the conference held 2-6 October, 2017 in Flagstaff, Arizona.

[84] Van Camp, M., de Viron O., Watlet A., Meurers B., Francis O., Caudron C.,
The gravity of geophysics
EOS, 98 (2017). DOI: 10.1029/2018EO086407

[85] Van Camp, M., de Viron, O., Watlet, A., Meurers, B., Francis, O., Caudron, C.
Geophysics from terrestrial time-variable gravity measurements
Reviews of Geophysics (2017). DOI: 10.1002/2017RG000566

[86] Van Camp, M., Francis, O., Lecocq, T.
Recording Belgium's Gravitational History
EOS, 98 (2017). DOI: 10.1029/2017EO089743

[87] Van Hove B., Karatekin Ö.
Atmospheric Reconstruction with Stagnation Pressure Flight Data from Mars Science Laboratory
Journal of Spacecraft & Rockets, Vol. 54, No. 3, May–June 2017.

[88] Van Noten, K., Lecocq, T., Sira, C., Hinzen, K., Camelbeeck, T.
Path and site effects deduced from merged transfrontier internet macroseismic data of two recent M4 earthquakes in NW Europe using a grid cell approach
Solid Earth, 8, pp. 453-477 (2017). DOI: 10.5194/se-8-453-2017

[89] Vanneste, K., Camelbeeck, T., Verbeeck, K., Demoulin, A.,
Morphotectonics and past large earthquakes in Eastern Belgium

A. Demoulin (ed.), Landscape and Landforms of Belgium and Luxemburg, World Geomorphological Landscapes, pp. 215-236 (2017). DOI: 10.1007/978-3-319-58239-9_13

[90] Verbeeck, K., Wouters, L., Vanneste, K., Camelbeeck, T., Vandenberghe, D., Beerten, K., Rogiers, B., Schiltz, M., Burow, C., Mees, F., De Grave, J., Vandenberghe, N.
Episodic activity of a dormant fault in tectonically stable Europe: The Rauw fault (NE Belgium)
Tectonophysics, 699, pp. 146-163 (2017). DOI: 10.1016/j.tecto.2017.01.023

[91] Verhulst, Tobias G. W. ; Stankov, Stanimir M.
Height-dependent sunrise and sunset: effects and implications of the varying times of occurrence for local ionospheric processes and modelling
Advances in Space Research, 60 issue 8, pp. 1797-1806 (2017). DOI: 10.1016/j.asr.2017.05.042.

[92] Williams R.J.R., Guzmán F., Badnell N.R., van Hoof P.A.M., Chatzikos M., Ferland G.J.
Thermodynamically consistent semiclassical l-changing rates
J. Phys. B, 50, 115201 (2017).

[93] Yseboodt, M., Dehant V., Péters M.J.
Signatures of the Martian rotation parameters in the Doppler and range observables
Planetary and Space Science 144, 74–88, (2017). DOI: 10.1016/j.pss.2017.05.008

[94] Zender, J., Kariyappa, R., Giono, G., Bergmann, M., Delouille, V., Damé, L., Hochedez, J-F., Kumara, S. T.
Segmentation of photospheric magnetic elements corresponding to coronal features to understand the EUV and UV irradiance variability
Astronomy & Astrophysics, 605 (2017). DOI: 10.1051/0004-6361/201629924

[95] Zhu P., Rivoldini A., Koot L., Dehant V.
Basic Earth's Parameters as estimated from VLBI observations
Geodesy and Geodynamics, 8, pp. 427-432 (2017). DOI: 10.1016/j.geog.2017.04.007

[96] Zorec J., Rieutord M., Espinosa Lara F., Frémat Y., Domiciano de Souza A. and Royer F.
Gravity darkening in stars with surface differential rotation
Astronomy and Astrophysics, 606, A32 (2017).

[97] Zorec J., Frémat Y., Domiciano de Souza A., Royer F., Cidale L., Hubert A.-M., Semaan T., Martayan C., Cochetti Y. R., Arias M. L., Aidelman Y. and Stee P.
Critical study of the distribution of rotational velocities of Be stars. II: Differential rotation and some hidden effects interfering with the interpretation of the V sin I parameter
Astronomy and Astrophysics, 602, A83 (2017).

Publications without peer review

[98] Asmar S.W., Armstrong J.W., Atkinson D.H., Bell D.J., Bird M.K., Dehant V., Iess L., Lazio T J.W., Linscott I.R., Mannucci A.J., Mazarico E., Park R.S, Patzold M., Preston R.A., Simpson R.A.
The Future of Planetary Atmospheric, Surface, and Interior Science Using Radio and Laser Links
Planetary Science Vision 2050 Workshop, held 27-28 February and 1 March, 2017 in Washington, DC. LPI Contribution No. 1989, id.8181.

[99] Baland R.-M., Yseboodt M., Van Hoolst T., Rivoldini A.
The influence of the fluid outer core and of the solid inner core on the orientation of the rotation axis of Mercury
ESPC Abstracts, EPSC2017-521-1, (2017).

[100] Banerdt W.B., Smrekar S., Hoffman T., Spath S., Lognonné P., Spohn T., Stone H., Willis J., Feldman J., De Paula R., Turner R., Asmar S., Banfield D., Christensen U., Clinton J., Dehant V., Folkner W., Garcia R., Giardini D., Golombek M., Grott M., Hudson T., Johnson C., Kargl G., Knapmeyer-Endrun B., Maki J., Mimoun D., Mocquet A., Morgan P., Panning M., Pike W.T., Russell C., Teanby N., Tromp J., Weber R., Wieczorek M., Hurst K., Barrett E. and the InSight Team
The InSight Mission for 2018
48th Lunar and Planetary Science Conference 2017, March 20-24, 2017 in The Woodlands, Texas, LPI Contribution No. 1964, id.1896.

[101] Berlanas, S. R., Herrero, A., Martins, F., Simón-Díaz, S., Mahy, L., Blomme, R. and the GES WG-13
Early-type massive stars in Carina Nebula within the Gaia-ESO Survey
Highlights on Spanish Astrophysics IX, ISBN 978-84-617-8931-3. S. Arribas, et al. (eds.), 453 (2017).

[102] Bettanini C., Esposito R., Debei S., Molfese C., Colombatti G., Aboudan A., Brucato J. R., Cortecchia F., Di Achille G., Guizzo G. P., Friso E., Ferri F., Marty L., Mennella V., Molinaro R., Schipani P., Silvestro S., Mugnuolo R., Pirrotta S., Marchetti E., Harri A.-M., Montmessin F., Wilson C., Arruego Rodriguez I., Abbaki S., Apestigue V., Bellucci G., Berthelier J. J., Calcutt S. B., Forget F., Genzer M., Gilbert P., Haukka H., Jimenez J. J., Jimenez S., Josset J. L., Karatekin, Ö., Landis G., Lorenz R., Martinez J., Möhlmann D., Moirin D., Palomba E., Pateli M., Pommereau J.-P., Popa C. I., Rafkin S., Rannou P., Renno N. O., Schmidt W., Simoes F., Spiga A., Valero F., Vazquez L., Vivat F., Witasse O.
The DREAMS experiment flown on the ExoMars 2016 mission for the study of Martian environment during the dust storm season
IEEE Metrology for Aerospace (MetroAeroSpace) pp.249-255 (2017).

[103] Blomme, R., Edvardsson, B., Eriksson, K., Frémat, Y., Korn, A., Lobel, A., Sordo, R., Thévenin, F.
StarNormal synthetic spectra used by CU6
Gaia Technical Note, GAIA-C6-TN-ROB-RHB-005-1 (2017-04-21).

[104] Bruyninx C., Araszkiewicz A., Brockmann E., Kenyeres A., Pacione R., Söhne W., Stangl G., Szafranek K., Völksen C.
EPN Regional Network Associate Analysis Center Technical Report 2016
In International GNSS Service Technical Report 2016, Eds Y. Jean, R. Dach, Astr.Inst. Univ. Bern, pp. 95-103 (2017). DOI: 10.7892/boris.99278

[105] Chehlaeh, N., Lampens, P., Mkrtichian, D., Van Cauteren, P., Vermeylen, L., Komonjinda, S.
Physical properties of the Algol-type eclipsing binary AO Ser
Journal of Physics Conference Ser. 901(1):012007, Siam Physics Congress 2017. DOI: 10.1088/1742-6596/901/1/012007

[106] De Cat, P.
Pulsating variable stars and large spectroscopic surveys
EPJ Web of Conferences, 152 issue id. 04001, pp. 1-12 (2017). DOI: 10.1051/epjconf/201715204001

[107] Defraigne P., Bertrand B., Huang W., Rovera D.,
Validation of the Inter-Frequency Calibration of Timing GNSS Receivers
proc. EFTF 2017, Besançon, 10-17 July 2017.

[108] Defraigne P., Huang W., Suard N., Kanj A., Delporte J., Marechal J., Uhrich P., Tuckey Ph., Sesia I., Signorile G.,
EGNOS Time and UTC disseminated by EGNOS
Proc. PTTI, Monterey, January 2017.

[109] Defraigne P., Tavella P., Sesia I., Cerretto G., Signorile G., Calonico D., Costa R., Clivati C., Cantoni E., De Stefano C., Frittelli M., Formichella V., Biserni E., Leone V., Zarroli E., Sormani D., Gandara M., Hamoniaux V., Varriale E., Morante Q., Widomski T., Kaczmarek J., Uzycki J., Borgulski K., Olbrysz P., Kowalski J., Cernigliaro A., Fiasca F., Perucca A., Dhiri V., Veiga M.T., Suárez T., Diaz J., Mangiantini M., Wallin MIKES Metrology A.E., Galleani L., Hindley D.
Demonstrator of Time Services based on European GNSS signals: the H2020 DEMETRA Project
Proc. PTTI, Monterey, January 2017.

[110] Dehant V., Le Maistre S., Baland R. M., Yseboodt M., Peters M. J., Karatekin O., Van Hove B., Rivoldini A., Baland R.-M., Van Hoolst T.
ExoMars Lander Radioscience LaRa, a Space Geodesy Experiment to Mars.
EGU General Assembly Conference Abstracts, volume 19, page 19305, April 2017.

[111] Dehant V., Le Maistre S., Baland R. M., Yseboodt M., Peters M. J., Karatekin O., Rivoldini A. Van Hoolst T.
ExoMars Lander Radioscience LaRa, a Space Geodesy Experiment to Mars
European Planetary Science Congress 2017, held 17-22 September, 2017 in Riga Latvia, extended abstract, id. EPSC2017-852.

[112] Elst E., Debehogne H.
6 positions of asteroids
MPS 815697 (2017).

[113] Fedorets, G., Muinonen, K., Pauwels, T., Granvik, N., Tanga, P.
Optimizing initial asteroid orbit determination of Gaia with normal point calculation
European Planetary Science Congress 2017, EPSC2017957.

[114] Ferri, F., Ahondan A., Colombatti, G., Bettanini C., Bebei S., Karatekin, Ö., Van Hove B., Gerbal, N., Asmar, S.
Atmospheric mars entry and landing investigations & analysis (AMELIA) by ExoMars 2016 Schiaparelli Entry Descent module: The ExoMars entry, descent and landing science
IEEE Metrology for Aerospace (MetroAeroSpace), pp 262-265 (2017).

[115] Frémat, Y., Marchal, O., Gosset, E., Lobel, A., Zorec, J.
Catalogue of Emission Line Stars and validation of GR2 data
Gaia Technical Note, GAIA-C6-TN-ROB-YF-008-1 (2017-05-18).

[116] Fu J.N., De Cat P., Smith M.
Synergies between spectroscopic and time-series photometric surveys - LAMOST observations for the Kepler field and K2 fields
American Astronomical Society Meeting 229, 305.02 (2017).

[117] Gloesener E., Karatekin Ö., Dehant V.
CH4-rich Clathrate Hydrate Stability Zone in the present Martian Subsurface
6th Mars Atmosphere Modelling and Observation (MAMO) Workshop, extended abstract, 17-20 January 2017, 3 pages (2017).

[118] Hakim K., Rivoldini A., Cottenier S., Van Hoolst T., Chust T. C., Steinle-Neumann G.
A new ab initio Equation of State of hcp-iron and its application to the interior structure of rocky super-Earths
48th Lunar and Planetary Science Conference, The Woodlands, Texas, U.S.A., March 20-24, 2017.

[119] Halain, J.-P., Berghmans, D., Defise, J.-F., Rochus, P., Nicula, B., de Groof, A., Seaton, D.
Performances of swap on-board PROBA-2
Proceedings of the SPIE, Volume 10565, id. 105650S 7 pp. (2017). DOI: 10.1117/12.2309237

[120] Halain, J.P., Mazzoli, A., Rochus, P., Renotte, E., Stockmans, Y., Berghmans, D., BenMoussa, A., Auchère, F.
EUV high resolution imager on-board solar orbiter: optical design and detector performances
Proceedings of the SPIE, 10564 issue id. 105643V 6 (2017). DOI: 10.1117/12.2309019

[121] Hrivnak B. J., Van Winckel, H. Van de Steene G.C., Bohlender D., Sperauskas J., Wenxian L.
Where are the binaries in proto-planetary nebulae? Results of a long-term radial velocity study
Proceedings of the IAU Symp. 323: "Planetary nebulae: Multi-wavelength probes of stellar and galactic evolution", eds. X.-W. Liu, L. Stanghellini and A. Karakas (2017).

[122] Irrgang A., De Cat P., Tkachenko A.
The evolved slowly pulsating B star 18 Peg. A testbed for upper main sequence stellar evolution
EPJ Web of Conferences, 152 issue id. 05010, pp. 1-2 (2017). DOI: 10.1051/epjconf/201715205010

[123] Irrgang A., De Cat P., Tkachenko A., Desphande A., Moehler S., Mugrauer M., Janousch D.
The evolved slowly pulsating B star 18 Peg: A testbed for upper main sequence stellar evolution
Proceedings of the Polish Astronomomical Society 5, 145 (2017).

[124] Jiang Z., Matsakis D., Zhang V., Achkar J., Arias F., Defraigne P., Dierik E., Esteban H., Fujieda M., Galindo F. J., Gotoh T., Jaldehag K., Jarlemark P., Liang K., Lin C., Mitchell S., Nawrocki J., Parker T., Petit G., Rieck C., Rovera G. D., Sesia I., Schlunegger C., Uhrich P., Wu W.
Long-term instability in UTC time links
Proc. PTTI, Monterey, January 2017.

[125] Karatekin Ö., Dehant V., Folkner W.M., LeMaistre S., Asmar S., Konopliv A.
Radioscience experiments to monitor atmospheric angular momentum variations onboard the forthcoming 2018 InSight and 2020 ExoMars landers
6th Mars Atmosphere Modelling and Observation (MAMO) Workshop, extended abstract, 17-20 January 2017, 3 pages (2017).

[126] Laguerre R., Cébron D., Noir J., Schaeffer N., Dehant V.
Dynamo driven by a precessing planet with an inner core
European Planetary Science Congress 2017, held 17-22 September, 2017 in Riga Latvia, extended abstract, id. EPSC2017-935.

[127] Lampens, P, Van Cauteren, P.
About DR UMa or the CRTS transient CSS110402:135906+554432
The Astronomer's Telegram issue 10220 (2017).

[128] Lampens, P., Van Cauteren, P.
Observations of AGN's
AAVSO AGN Circulars dd. 18 Jan, 1 Mar, 8 Mar, 15 Mar, 12 Apr (53 obs. in total) (2017).

[129] Lecocq, T., Camelbeeck, C.
Electrical resistivity tomography data across the Hockai Fault Zone (Ardenne, Belgium)
Data in Brief, 11, pp. 1-4 (2017).

[130] Lobel, A.
Pianoconcerto voor Gele Hyperreus Rho Cassiopeiae
Zenit, 2017 May Issue on Massive Stars (in Dutch) (2017).

[131] Lobel, A., Martayan, C., Mehner, A., Groh, J.,
Modelling and observations of massive binaries with the B[e] phenomenon
in 'The B[e] Phenomenon : Forty Years of Studies', eds. A. Miroshnichenko, S. Zharikov, and D. Korcakova, ASP Conf. Ser., Vol. 508.

[132] Meftah, M., Dominique, M., BenMoussa, A., Dammasch, I., Bolsée, D., Pereira, N., Damé, L., Bekki, S., Hauchecorne, A.
On-orbit degradation of recent space-based solar instruments and understanding of the degradation processes
Proceedings of the SPIE, 10196 (2017). DOI: 10.1117/12.2250031

[133] Molenda-Żakowicz J., Frasca A., De Cat P., Catanzaro G.
The LAMOST spectroscopic survey of stars in the Kepler field of view: Activity indicators and stellar parameters
EPJ Web of Conferences, 152, issue id. 04002, pp. 1-5 (2017).

[134] O'Rourke J. G., Gillmann C. and Tackley P.
Prospects for an Ancient Dynamo and Modern Crustal Remnant Magnetism on Venus
15th Meeting of the Venus Exploration and Analysis Group (VEXAG), held 14-16 November, 2017 in Laurel, Maryland.

[135] Paladini C., Klotz D., Sacuto S., Lagadec E., Wittkowski M., Richichi A., Hron J., Jorissen A., Groenewegen M.A.T., Kerschbaum F., Verhoelst T., Rau G., Olofsson H., Zhao-Geisler R., Matter A.
To be or not to be Asymmetric? VLTI/MIDI and the Mass-loss Geometry of AGB Stars
in: ESO Messenger 168, 28 (2017).

[136] Ritter, B., Karatekin, Ö., Gerbal, N., Van Hove, B., Carrasco, J., Ranvier, S., De Keyser, J.
SOLVE: a small spacecraft for near lunar environment exploration
European Planetary Science Congress 2017, held 17-22 September, 2017 in Riga Latvia, id. EPSC2017-622.

[137] Rivoldini A., Deproost M.-H., Van Hoolst T., Baland R.-M., Yseboodt M., Le Maistre S., Péters M.-J., Dehant V.
Constraints on the interior structure of Mars from nutations
European Planetary Science Congress 2017, held 17-22 September, 2017 in Riga Latvia, extended abstract, id. EPSC2017-755.

[138] Stein, S., Spencer, B., Vanneste, K., Camelbeeck, T., Vleminckx, B.
Assessing how well earthquake hazard maps work: Insights from Weather and Baseball
Earth Magazine, March 2017, pp. 36-41 (2017).

[139] Stockman, Y., BenMoussa, A., Dammasch, I., Defise, J.-M., Dominique, M., Halain, J.-P., Hochedez, J.-F., Koller, S., Schmutz, W., Schühle, U.
In-flight performance of the solar UV radiometer LYRA/PROBA-2
Proceedings of the SPIE, Volume 10565, id. 105650A 7 pp. (2017). DOI: 10.1117/12.2309149

[140] Stockman, Y., Hochedez, J.-F., Schmutz, W., BenMoussa, A., Defise, J.-M., Denis, F.; D'Olieslaeger, M., Dominique, M., Haenen, K., Halain, J.-P., Koller, S., Koizumi, S., Mortet, V., Rochus, P., Schühle, U., Soltani, A., Theissen, A.
LYRA, solar uv radiometer on the technology demonstration platform PROBA-2
Proceedings of the SPIE, Volume 10567, id. 105673K 7 pp. (2017). DOI: 10.1117/12.2308059

[141] Tavella P., Sesia I., Cerretto G., Signorile G., Calonico D., Costa R., Clivati C., Cantoni E., Defraigne P., De Stefano C., Frittelli M., Formichella V., Biserni E., Leone V., Zarroli E., Sormani D., Gandara M., Hamoniaux V., Varriale E., Morante Q., Widomski T., Kaczmarek J., Uzycki J., Borgulski K., Olbrysz P., Kowalski J., Cernigliaro A., Fiasca F., Perucca A., Dhiri V., Veiga M.T., Suárez T., Diaz J., Mangiantini M., Wallin A.E., Galleani L., Hindley D.
The H2020 European Project DEMETRA: Experimental Time Services based on European GNSS Signals
proc. EFTF 2017, Besançon, 10-17 July 2017.

[142] Turbet M., Forget F., Svetsov V., Popova O., Gillmann C., Karatekin O., Wallemacq Q., Head J.W., Wordsworth R.
Catastrophic Events: Possible Solutions to the Early Mars Enigma(s)?
Sixth International Workshop on the Mars Atmosphere: Modelling and observation, Granada, Spain, January 17-20 2017.

[143] Van de Steene G. C.
Herschel observations of planetary nebulae
Proceedings of the IAU Symp. 323: "Planetary nebulae: Multi-wavelength probes of stellar and galactic evolution", eds. X.-W. Liu, L. Stanghellini and A. Karakas (2017).

[144] Van de Steene G.C., van Hoof P.A.M., Kimeswenger S., Zijlstra A.A., Avison A., Guzman-Ramirez L., Hajduk M., Herwig F.
The very fast evolution of Sakurai's object
Proceedings of the IAU Symp. 323: "Planetary nebulae: Multi-wavelength probes of stellar and galactic evolution", eds. X.-W. Liu, L. Stanghellini and A. Karakas, p. 380 (2017).

[145] van Hoof P.A.M., Herwig F., Kimeswenger S., Van de Steene G.C., Avison A., Zijlstra A.A., Hajduk M., Guzmán-Ramirez L., Woodward P.R.
The i process in the post-AGB star V4334 Sgr
Mem. S.A.It., 88, 463 (2017).

[146] Van Malderen, R., Pottiaux, E., Klos, A., Bock, O., Bogusz, J., Chimani, B., Elias, M., Gruszczynska, M., Guijarro, J., Zengin Kazancı, S., Ning, T.
Homogenizing GPS Integrated Water Vapour Time Series: Methodology and Benchmarking the Algorithms on Synthetic Datasets
Proceedings of the Ninth Seminar for Homogenization and Quality Control in Climatological Databases and Fourth Conference on Spatial Interpolation Techniques in Climatology and Meteorology, pp. 104-116 (2017).

[147] Vansintjan, R.
The SOLARNET Solar Virtual Observatory prototype
SOLARNET IV: The Physics of the Sun from the Interior to the Outer Atmosphere, held 16-20 January 2017 in Lanzarote, Spain. Online at http://www.iac.es/congreso/solarnet-4meeting, id.91.

[148] Verbeeck C., Stegen K.
What can EUI do for you?: onboard science programs
Talk presented at 20th EUI Consortium Meeting, MSSL, Guildford, UK, September 13-15, 2017 on 2017-09-15.

[149] Yseboodt M., Dehant V., Baland R.M.
Mars rotation using geodesy data
American Astronomical Society, DDA meeting #48, London, United Kingdom, 11-15 June 2017, extended abstract, id.202.03.

Other publications (books, book chapters…)

[150] Defraigne P.
GNSS Time and Frequency Transfer
Springer Handbook of Global Navigation Satellite Systems, Editors: Teunissen, Peter J.G., Montenbruck, Oliver (Eds.), 2017.

[151] Delouille, V., Hofmeister, S., Reiss M., Mampaey B., Temmer M. and Veronig, A.
Coronal Hole detection using supervised classification
Machine Learning Techniques for Space Weather, 2018, Elsevier.

[152] Pauwels, T., Bruyninx, C., Cuypers, J., Roosbeek, F.
Annuaire de l'Observatoire royal de Belgique – Jaarboek van de Koninklijke Sterrenwacht van België 2018
Fedopress, ISSN 03734900 (2017).

[153] Van Noten, K., Burlet, C., Delaby, S., Verheyden, S., Lecocq, T.
Investigations géophysiques du remplissage sédimentaire de la Salle de la structure
in Grotte de Bruniquel (Bruniquel, Tarn-et-Garonne). Rapport d'opération archéologique programmée 2017. (Sc. Ed. Jaubert, J., Verhyden, S. and Soulier, M. - pp. 135-143).

Annex 2: Workforce

At the end of 2017, 172 employees are working in the Royal Observatory of Belgium (comprising people working at the Planetarium).

Here are some representative statistics of the personnel in 2017.

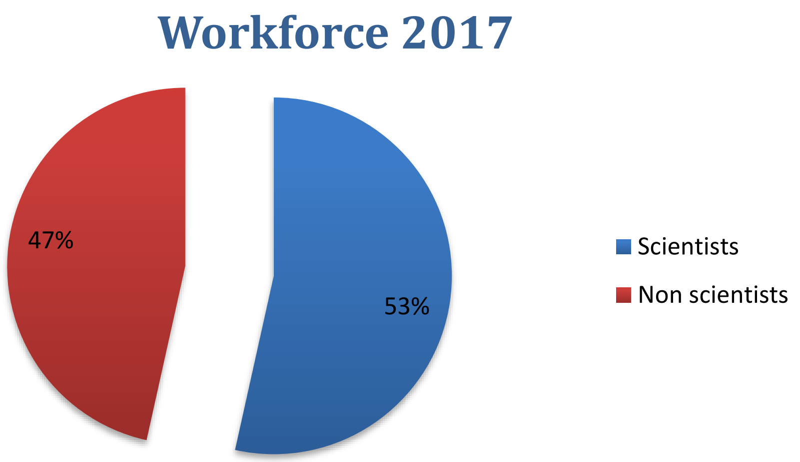

59 people of the staff are women and 113 are men. As expected from a research institute, scientists constitute the main part of the personnel (92 agents).

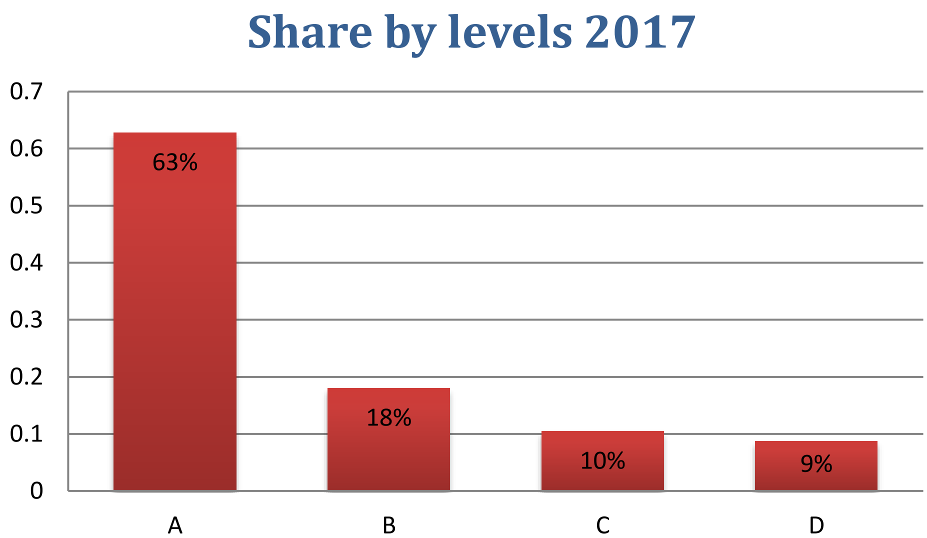

Moreover, a high percentage (63 %) of the Royal Observatory of Belgium personnel has a university-level function (scientific or of A-level). This is mainly due to the fact that the Observatory is a research institute whose main activity is the production of scientific knowledge and expertise.

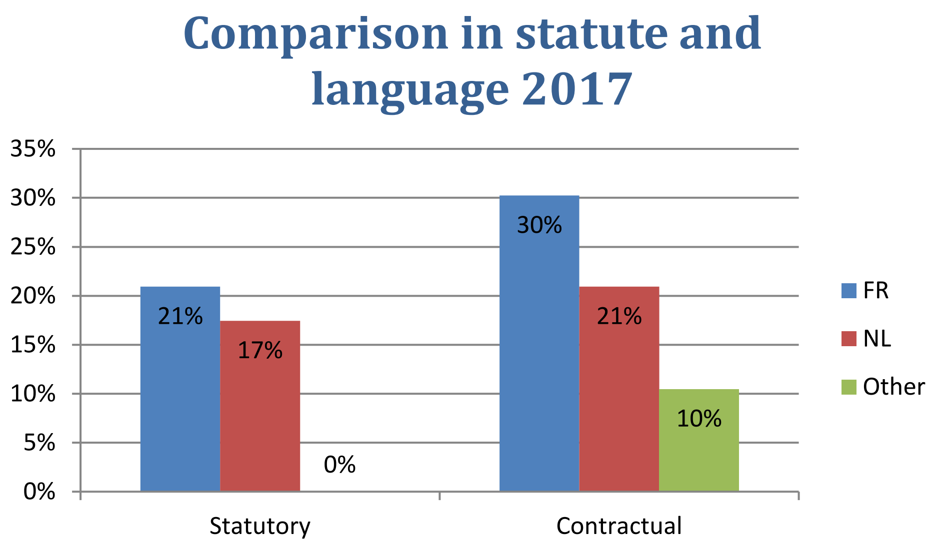

62% of the personnel are contractual. 38 % Dutch-speaking people and 51 % are French-speaking people. 18 members of the scientific personnel (about 10 % of the staff), all of which being contractual, have a master in a different language than French and Dutch. This reflects the international character of the scientific environment.